NUREG/CR—4558
SAND85—1739
R5, R7
Printed June 1986

Interaction of Hot Solid Core Debris With Concrete

E. R. Copus, D. R. Bradley

Prepared by
Sandia National Laboratories
Albuquerque, New Mexico 87185 and Livermore, California 94550
for the United States Department of Energy
under Contract DE-AC04-76DP00789

Prepared for
U. S. NUCLEAR REGULATORY COMMISSION

SF2900Q(8-81)

Available from

Superintendent of Documents
U.S. Government Printing Office
Post Office Box 37082
Washington, D.C. 20013-7982

and

National Technical Information Service
Springfield, VA 22161

NUREG/CR-4558
SAND85-1739
R5,R7

INTERACTION OF HOT SOLID CORE DEBRIS WITH CONCRETE

E. R. Copus
D. R. Bradley

NUREG/CR--4558

TI86 015849

June 1986

Sandia National Laboratories
Albuquerque, NM 87185
operated by
Sandia Corporation
for the
U.S. Department of Energy

Division of Accident Evaluation
Office of Nuclear Regulatory Research
U.S. Nuclear Regulatory Commission
Washington, DC 20555
Under Memorandum of Understanding DOE 40-550-75
NRC FIN No. A 1218

ABSTRACT

The Hot Solid program is intended to measure, model, and assess the thermal, gas evolution, and fission product source terms produced as a consequence of hot, solid, core debris-concrete interactions. Two preliminary experiments, HSS-1 and HSS-3, were performed in order to compare hot solid UO_2-concrete and hot solid steel-concrete interactions. The HSS-1 experiment ablated 6 cm of limestone-common sand concrete in a little more than three hours using a 9 kg slug of 304 stainless steel at an average debris temperature of 1350°C. The HSS-3 experiment ablated 6.5 cm of limestone-common sand concrete in four hours using a 10 kg slug of 80% UO_2-20% ZrO_2 at an average debris temperature of 1650°C. Both experiments were inductively heated and contained in a 22 cm alumina sleeve to simulate one-dimensional axial erosion. The HOTROX computer code model was evaluated using the results from the HSS tests. HOTROX is a 1-D concrete ablation model that calculates transient conduction and gas release in the concrete as well as heatup of the hot solid slug. Using the HSS-1 power input history and geometry, HOTROX calculates 6.2 cm of concrete erosion in 200 minutes. Using the HSS-3 input conditions, HOTROX predicts 6.8 cm of erosion in 190 minutes. These results compare favorably with the experimental erosion rates. The calculated thermal response of the concrete is also close to experimentally measured values. The information from the Hot Solid Program will be used both to expand the post-accident phenomena data base and to extend the range of applicability of current accident analysis computer models such as CORCON and CONTAIN.

TABLE OF CONTENTS

LIST OF FIGURES

LIST OF TABLES

I. INTRODUCTION

The Hot Solid Program is an ongoing experimental project at Sandia National Laboratories. The objective of the Hot Solid Program is to measure, model, and assess the long-term interactions of solid core debris with concrete. This type of long-term interaction, which includes basemat erosion, flammable and non-flammable gas evolution, long-term fission product release, and the overall core-concrete heat balance, will occur following a catastrophic core melt accident when degraded core materials solidify after prolonged contact with the concrete basemat. It will also occur when an ex-vessel steam explosion forms a fragmented core debris bed. The thermal, gas evolution, and fission product source terms produced as a consequence of hot solid core-concrete interactions are the governing phenomena in any long term postaccident containment integrity evaluation or risk/consequence analysis. At present, the data base and computer models[1,2] used to postulate the potential postaccident containment failure probability and associated consequences include only short-term transient effects of core debris/concrete interactions at temperatures and heat fluxes resulting from decay heat powers greater than 0.5 W/g. The Hot Solids program will measure, model, and assess the thermal, gas evolution, and fission product source terms that result from decay heat powers in the 0.1 to 0.01 W/g range. This information will be used both to expand the present postaccident phenomena data base and to extend the range of current accident analysis computer models such as CORCON[7] and MEDICI[9] so that long term core-concrete interactions are included in addition to the short-term transient effects.

In order to expand the data base and extend current computer models, four variables are of primary interest and importance: debris configuration, concrete composition, decay heat power, and coolant interactions. Variables of secondary interest include geometric scaling factors and fission product transport mechanisms. Experiments within the Hot Solid Program will include both base case experiments intended to develop extended computer models and follow-on experiments intended to assess those models and expand the data base. Base case experiments will be conducted using inductively heated metallic steel and oxidic UO_2 debris on limestone concrete in a small scale 1-D crucible configuration at effective power levels varying from 0.1 to 0.01 W/g. Data from these experiments will describe and correlate radial and axial concrete erosion, total gas production, flammable gas production, fission product distribution, and the global debris concrete heat balance (including coolant interaction effects) as a function of time, temperature, and heat flux. These descriptions and correlations will be used to develop a computer model compatible with CORCON and other safety analysis codes, which will include convective, conductive, and radiative heat transfer mechanisms. It will also be capable of describing the core debris as a porous solid and will carry the core

concrete reaction to an effective termination point at which time all erosion, gas evolution, and fission product release cease. This model will be a distinct improvement over current models that use convection as the primary heat transfer mechanism, describe the core debris as either a liquid or a non porous monolith, and terminate the core-concrete interaction either prematurely or not at all.

Finally, the computer model developed using these initial base case Hot Solid tests will be exercised, evaluated, and extended to reactor scale geometries. This will be done with follow-on experiments using larger 2-D geometries, different concrete types, and fragmented core debris. These experiments will be used to exercise the base case 1-D model, to evaluate the effects of scaling up that model to intermediate and large scale safety analyses, and to expand the postaccident interaction phenomena data base.

II. BACKGROUND

In the unlikely event of a reactor core meltdown that is followed by failure of the reactor pressure vessel, the interaction of core debris with the concrete basemat can occur. Although the probability of this type of accident is small,[1] an assessment of the interaction is desirable for the proper evaluation of the risks of nuclear power. The interaction of core debris heated internally by the decay of fission products with structural concrete has been identified as a little understood aspect of such accidents.[2]

Following melt-through of the reactor pressure vessel, the accident may proceed in several different directions. If coolant is present in the reactor cavity, the molten core material may cause a steam explosion that fragments all or part of the melt.[3] The Zion and Indian Point Probabilistic Safety Studies[4,5] propose additional fragmentation mechanisms that may be operative instead of, or in combination with, a steam explosion. Rapid quenching of the melt will accompany extensive fragmentation and the core material will exist as a debris bed cooled by the remaining water in the cavity. Depending on the configuration of the debris (e.g., bed height and particle size) and the decay power generated in the bed, localized dryout and remelting can occur.[6] If, on the other hand, heat transfer within the debris is sufficient to prevent remelting, the accident will proceed as a hot solid interaction with concrete. The ZPSS and IPPSS reports also indicate that rapid quenching of the melt may occur even if no fragmentation takes place, as long as sufficient coolant is present in the cavity. Here again the core debris would interact with the concrete in the form of an internally heated solid material.

Vastly different accident scenarios can result if no coolant is present in the reactor cavity at the time of pressure vessel

melt-through. Here no fragmentation or quenching occurs and the molten core material begins to interact with the concrete immediately. As the concrete is heated and subsequently ablates, steam and carbon dioxide are released in sufficient quantity to cause vigorous stirring of the melt.[11] Although some analyses assume that the melt rapidly becomes stratified into separate oxidic and metallic layers[7] (which would be the case in a quiescent pool), some experimental results indicate that the two phases are intermixed by the gas stirring.[8] Regardless of the configuration of the melt, its decay power will eventually drop and the melt will solidify. In this scenario, as in the previous one, the long-term phase of the reactor accident is governed by the interaction of hot solid core debris with structural concrete.

Regardless of whether the core debris is molten or solidified, fragmented or monolithic, there are several phenomena that must be well understood before the ex-vessel phase of the accident can be assessed. The following is a list of those phenomena that have the greatest influence on the progression of a core-concrete interaction and its related risk evaluation:

1. heat transfer to the concrete and to the containment atmosphere,
2. heat conduction in the concrete,
3. gas release from the concrete and corresponding changes in concrete properties,
4. reduction of these gases (H_2O and CO_2) as they pass through the debris,
5. ablation (melting) of the concrete,
6. transport of the molten concrete/released gas mixture,
7. crust and/or slurry formation as the molten debris cools (transition to the hot solid-concrete interaction),
8. fission product redistribution within the debris,
9. aerosol production during the core-concrete interaction, and
10. accident termination either by coolant addition or natural cooling.

The driving force in the interaction is the rate at which heat is transferred to the concrete. As the concrete heats up, several of its constituents (e.g., $CaCO_3$, $Ca(OH)_2$) undergo chemical reactions that liberate steam and carbon dioxide. In addition to this, free water that has remained in the pores of the concrete evaporates, providing another source of steam. As these concrete decomposition events occur, gas is released and thermophysical properties change. Most important of these are the concrete density, specific heat, and thermal conductivity. As the concrete temperature continues to rise, its chemical components begin to melt. Once melted, the concrete is quickly displaced from the debris-concrete interface by the combined force of the weight of the debris and the flow of released gas.

The ultimate location of this slag material will affect the long-term heat transfer characteristics of the debris. For example, if a slag crust forms at the top surface of the debris, it will reduce radiation heat loss and may also prevent the debris from being quenched by coolant, which is added later.

The core-concrete interaction influences not only the containment structure adjacent to the debris, but also the containment atmosphere above the debris. The concern here is the ability of the containment to withstand the long-term pressurization that occurs during the interaction. The pressure increases both as a result of direct heating of the atmosphere by the debris and released aerosols, and also by the addition of non-condensable gases produced during concrete decomposition. As released H_2O and CO_2 pass upward through the debris, they are reduced to H_2 and CO by oxidation of the metallic components of the debris. These two gases not only add to the pressure in the containment, but because they are flammable they may cause rapid overpressurization and failure of the containment if ignited. If the containment fails, the risk to the public is greatly affected by the magnitude and nature of the aerosols released during the interaction.

Based on previous experimental work at Sandia,[9,11] aerosol production appears to be a strong function of the debris temperature and the net heat flux to the concrete. When the debris is molten and very hot, dense aerosol clouds have been observed, while for lower temperature, solid debris, aerosol production appears to be much smaller.

The composition of these aerosols is also of great importance, especially with respect to their radioactive fission product content. Related to this is the question of fission product redistribution within the debris. Fission products that partition into the concrete slag layer on the top of the debris have a much greater probability of release in aerosol form than if they reside well below the surface.

Another question related to fission product relocation is the distribution of decay heat within the debris. Correct thermal modeling of a core-concrete interaction requires an a priori knowledge of the location and magnitude of the energy sources within the debris. This is another aspect of the interaction about which more data are required.

Finally, of special concern is the question of when the core-concrete interaction terminates; namely, how long will the interaction proceed and is it possible to quench the debris and thus stop the interaction by adding coolant to the reactor cavity. Current severe accident scenarios are open-ended, i.e., once the core-concrete interaction has begun, it is assumed to continue for some unspecified period of time. Eventually, decay heat generation within the core debris will drop to a level where

the accident will terminate naturally. However, it is not known whether the time required for this to occur is hours, days, weeks, or even months.[10] In order to insure against a "China Syndrome" type accident,[1] the concrete basemat must be thick enough to prevent complete penetration by the debris. If basemat penetration does occur, radioactive fission products can be transported through subsurface ground water. Other times of importance correspond to termination of CO_2/CO production and finally of H_2O/H_2 production. When gas production from core-concrete interactions ceases, the threat to containment integrity is reduced.

Prior to natural termination, it may be possible to stop the core-concrete interaction by introducing coolant into the reactor cavity. The heat removal capability of the coolant depends on several factors, the more obvious of which are the magnitude of the heat flux and the debris surface area available for heat transfer. If boiling heat transfer is assumed, the heat flux to the coolant can vary over at least an order of magnitude depending on the debris surface temperature and the subcooling of the coolant. Of even greater importance is the surface-to-volume ratio for the debris. For a deep, monolithic debris formation the available surface area may be small enough and the depth large enough that erosion of the concrete floor is essentially unaffected by the coolant. On the other hand, for a shallow, fragmented debris bed a quenched configuration might be maintained for a long period of time.

The goal of the Hot Solids program is the development and experimental verification of a computer model which incorporates all of the phenomena just mentioned. In order to understand how this effort meshes with our current level of knowledge, it is instructive to review both the existing data base and the models and computer codes presently in use. Experiments and models for both molten core-concrete and hot solid-concrete interactions will be examined. This will provide a better understanding of the transition between the two accident phases and how the results of the current effort might be incorporated into a single analytical tool which handles both.

A. Previous Experiments

Most previous experimental work has concentrated on the melt-concrete interaction phase of the accident.[11-16] Some experiments which used simulant materials were aimed at developing models for isolated aspects of the interaction (e.g. convective heat transfer in a bubbling pool) while other experiments used more prototypic materials in order to obtain qualitative information on the important phenomena during the interaction. In this latter group, some experiments were internally heated and sustained through induction or joule heating[13-16], while others were transient tests in which molten material

was teemed into concrete crucibles.[11,12] Most used melts composed of steel or thermite[11-14], while others used molten UO_2.[15,16] Each was characterized by initial temperatures well above the ablation temperature of the concrete, which resulted in rapid gas production and concrete erosion, and quite often led to ignition of the flammable gases (H_2, CO, and CH_4) produced during oxidation of the melt. Large quantities of aerosols were often generated during these vigorous melt-concrete interactions.

Much less experimental work has been devoted to the more benign, but longer term interaction between hot solid core debris and concrete. Some work has been done with simulant materials - for example, heated steel balls penetrating an ice substrate[17] or a heated copper block penetrating a dry ice (solid CO_2) substrate[18] - but because they cannot match the unique characteristics of concrete (e.g., continuous release of H_2O and CO_2 and concurrent melting) only qualitative information can be gleaned from these tests. More valuable are the few hot solid-concrete tests which have been completed.[19-21] At Sandia National Laboratories, two tests in the BURN series exposed a concrete crucible to an inductively heated slug of mild steel weighing 5 kg. In the BURN2 experiment[19] the limestone-common sand concrete crucible began to erode when the steel temperature reached 1630 K and continued to erode as long as heating of the steel slug was sustained (approximately two hours). In the BURN3 experiment[20] a high carbonate, low silicate concrete was used for the crucible. Because of the very high liquidus temperature of this concrete (approximately 1875 K) no erosion occurred until after the steel had melted. As a result, only the premelting phase of the test was representative of a hot solid-concrete interaction. These two BURN tests were designed to demonstrate only that the core-concrete interaction continues long after the core debris has solidified and were therefore not heavily instrumented, follow-up testing was required.

The next major experimental effort was the recently completed FRAG test series.[21] In the FRAG tests 45 kg of 3-4 mm diameter mild steel spheres were inductively heated in crucibles made of basaltic or limestone-common sand concrete. Numerous thermocouples were used to monitor heatup of both the steel and the concrete. Gas release was monitored using an orifice plate to measure flow and grab samples were taken to determine gas composition. Videotape cameras were used to observe and record the progress of the experiments. In each FRAG test induction heating of the "debris" was sustained for at least two hours following incipient concrete erosion and in each case a crust formed when the molten concrete was transported through the debris by released gases and subsequently encountered a cooler region of the steel spheres. In the later two of the four FRAG tests water was added to the system after erosion began. In these two experiments, the water was prevented from reaching the lower portion of the debris by the presence of the crust, and concrete erosion was unabated. Such a result calls into question

the efficacy of using water to mitigate a fragmented core debris-concrete interaction. However direct scaling to reactor cavity dimensions is not possible[21] so further work must be done in this area. It was also observed that the H_2O and CO_2 released from the concrete were quickly reduced to equilibrium concentrations of H_2 and CO during the oxidation of the debris. This result should also apply in the reactor case though the equilibrium concentrations of the two flammable gases will differ from the experiments because of the different materials in the reactor core debris. These and other safety questions will be studied more thoroughly in the Hot Solids experimental program.

B. Previous Models

As with the experimental work in core-concrete interactions, most of the previous analytical work has involved only the melt-concrete phase of the accident. Recently, some attention has also been focused on the transition from molten core debris to completely solidified core debris and on the subsequent long term interaction of this hot solid material with the concrete basemat. In some cases, the goal of the analysis has been the development of an integral computer code which attempts to model all of the important phenomena occurring during the interaction, while in other cases the goal was an accurate representation of a single phenomenon (e.g., heat transfer to the concrete or concrete erosion). Especially with the integral computer codes, assumptions and approximations are often made either without any experimental validation or based on simulant experiments which may or may not be applicable to reactor accident conditions. Hence there is considerable uncertainty in the accuracy of the calculated results. In the combined experimental and analytical program discussed here the validity of the models which are developed will be established through comparison to experiments which use prototypic materials under prototypic thermal conditions.

In the following discussion, currently available models for core-concrete interactions are examined in some detail. Melt-concrete models are discussed first, followed by hot solid- concrete models, and finally recently developed models which attempt to handle both interaction phases. Table I provides a brief summary of the important features of these models.

B.1. Melt-Concrete Interaction Models

In the analysis of melt-concrete interactions, special attention has been, and continues to be devoted to models for heat transfer between the molten core debris and the concrete. The reason for this is that heat transfer to the concrete directly or indirectly drives every phase of the interaction from concrete ablation to aerosol and fission product release. Because the concrete releases a significant amount of gas (H_2O and CO_2) when it is heated, each of the models features heat transfer

mechanisms dominated by gas flow. At the melt-concrete interface the situation is analogous to either nucleate or film boiling depending on the gas flow rate. At high gas fluxes a stable gas film may exist thereby preventing direct contact between the molten debris and the concrete, while for lower gas fluxes a stable film is not possible and there will be intermittent contact between the melt and the concrete. While most of the convective heat transfer models presented in Table I assume the presence of a stable gas film[22-24] recent analytical work has been devoted to the intermittent contact regime.[25] In an actual melt-concrete interaction a stable gas film may exist for a period of time, but then as the melt cools the heat flux and gas flow rate may drop below that required to sustain the film. Hence, both regimes must be considered in order to accurately represent the interaction.

As mentioned earlier, a number of integral computer codes have been written to describe the important (from the standpoint of reactor safety) features of core melt-concrete interactions. While each attempts to model the same phenomena, they differ greatly in the assumptions and approximations they employ and as a result often produce quite different results for the same accident calculation. Because very few prototypic experiments have been performed to verify these codes, it is not possible to state without question which is most accurate. In the following paragraphs the four integral codes, INTER, CORCON-MOD1, GROWS2, and WECHSL will be discussed briefly. A summary of this discussion is provided by Table I.

The forerunner of the melt-concrete interaction codes was INTER which was developed at Sandia National Laboratories.[26] It modeled most of the important phenomena but used parametric rather than mechanistic models for much of the calculation. For this reason it was meant only as a first approximation to the melt-concrete interaction.

In INTER the melt pool is assumed to have the shape of a hemispherical segment intersected by a cylinder. The pool is allowed to expand as concrete erodes but the cavity shape is maintained in the same simple form. The molten debris is assumed to be stratified into an oxidic and metallic layer, with the less dense layer on top. Each layer is assumed to be solid or liquid depending on its temperature. Crust formation is not allowed. Heat transfer to the concrete is governed by a conduction-inspired boundary layer growth equation

$$\frac{d\delta}{dt} = 0.72 \frac{\alpha}{\delta}$$

Table I

Characteristics of Current Core-Concrete Models

Models (Refs.) / Phenomena/Geometry	Dhir, et. al (22)	Alsmeyer, et. al (23)	Blattner (4)	Lee et. al (25)	INTER (26)	CORCON MOD1	WECHSL (27)	GROWS2 (29)	Emerman & Turcotte (31)	Turland (32)	Ahmed & Dhir (18)	USINT (33)	Corradini (34)	Corradini (35)	CORCON-MOD2 (36)	DECOMP (37)	SLAM (38)
1-D Geometry										X	X	X	X				X
2-D Geometry					X	X	X	X						X	X	X	
Molten Debris	X	X	X	X	X	X	X	X		X					X	X	X
Solid Debris									X		X			X	X	X	
Convection	X	X	X	X	X	X	X	X	X		X				X	X	X
Radiation					X	X	X	X			X		X	X	X	X	X
Gas Film	X	X	X			X	X				X			X	X		
Albation/Melting					X	X	X	X	X	X	X		X	X	X	X	X
Conduction into Concrete					X			X		X		X	X	X		X	X
Gas Release					X	X	X	X			X	X	X		X	X	X
H_2O/CO Production					X	X	X								X	X	
Gross Mixing								X								X	X
Stratification					X	X	X								X		
Crust Formation								X							X	X	
Slurry Formation						X	X										
Boiling of Coolant															X	X	

where δ is the boundary layer thickness and α is the thermal diffusivity of the layer. The effective convection heat transfer coefficient is then calculated by

$$h = \frac{k}{\delta}$$

where k is the layer thermal conductivity. This formulation is subject to constraints which are applied with little justification. While INTER calculates heat conduction into the concrete (albeit in a much simplified fashion) it does not calculate gas release as a result of this heating. Instead the conducted energy is subtracted from that incident at the concrete surface to calculate a net heat flux for concrete ablation. Only gas contained in this ablated concrete is released and allowed to react chemically with the melt, thereby producing H_2 and CO. All chemical reactions are assumed to go to equilibrium.

The three other previously mentioned integral codes, CORCON-MOD1, GROWS2, and WECHSL, represent the second generation of melt-concrete interaction codes. Because CORCON-MOD1 and WECHSL are closely related, they will be discussed together. GROWS2 will be discussed separately.

CORCON-MOD1[1] and WECHSL[27] were developed concurrently at Sandia National Laboratories and Kernforschungszentrum Karlsruhe (KfK) in West Germany and have many of the same features. Both calculate general two-dimensional axisymmetric cavity geometries and assume stratified (oxidic and metallic) debris layers in the melt pool. Both use mechanistic (but different) convective heat transfer models which are based on results from simulant experiments. Neither treats transient conduction in the concrete and as a result both assume that all energy transferred to the concrete results in ablation. Both codes also calculate the reduction of H_2O and CO_2 to H_2 and CO by assuming that all chemical reactions proceed to equilibrium.

The most significant differences between CORCON and WECHSL lie in their treatment of heat transfer from the melt to the concrete. Here CORCON assumes that a stable gas film always separates the molten debris from the concrete regardless of the magnitude of the gas flow rate. Heat is transferred directly to the concrete from the melt by thermal radiation and indirectly by convection from the flowing gas. WECHSL also considers this mode of heat transfer but allows a transition to an intermittent contact mode when the gas film is no longer sustained. The criterion for transition used in the code is similar in form to Berenson's criterion[28] for the collapse of a stable boiling film. Because this transition is physically reasonable, WECHSL appears to offer a somewhat more realistic representation of heat transfer at the melt-concrete interface. The importance of this effect, however, is not presently known.

The GROWS2[29] computer code which was developed at Argonne National Laboratory is significantly different in most aspects from the three previously discussed codes. It treats the molten debris as a homogeneous mixture of core and substrate materials rather than as a stratified pool. The concrete cavity is assumed to always have a horizontal bottom surface and vertical sidewalls with a circular cross-section. Radial and axial erosion are then governed by independent heat transfer models for the two surfaces.

Overall heat transfer to the concrete is a combination of several different mechanisms. The following is a list of the mechanisms that are considered:

1. conduction through a stable horizontal inversion layer enhanced by internal thermal radiation,
2. natural convection at the sidewalls enhanced by internal thermal radiation,
3. energy transfer from soluble globules of molten concrete to the molten fuel debris, and
4. energy transfer as a result of gas bubbling through the melt.

Heat transfer coefficients for the different mechanisms are calculated separately (even though they may not be independent of one another) and are then combined to determine an overall coefficient according to the following equation:

$$h_{eff} = \left[\Sigma_i \, h_i^2\right]^{.5}$$

No justification for combining terms in this fashion has been given by the developers of the code.

One distinct advantage of the GROWS2 code is that it calculates transient conduction into the concrete and subsequent H_2O and CO_2 release when decomposition temperatures are reached. Since energy conducted away from the melt-concrete interface is not available for ablation, erosion of the concrete is much slower than that calculated by either CORCON or WECHSL. In a recently published comparison of CORCON and GROWS2 results for a sample accident calculation[30], thirty times more concrete volume was eroded in the CORCON calculation while the gas release results were virtually the same. This illustrates the necessity for including both transient conduction into the concrete and the resulting subsurface gas release. This is especially true when the molten debris begins to solidify and much lower conduction-limited heat fluxes govern the interaction.

B.2. Hot Solid-Concrete Interaction Models

Neglecting for the moment the transition from molten to solidified core debris, we will address now the long term inter-

action of solid core debris with concrete. Although a much more benign interaction, this phase of the accident may continue for a considerable length of time leading ultimately to containment failure by overpressurization or basemat penetration.

Until recently very little analytical effort has been devoted to the hot solid-concrete interaction. However, prior work in the areas of radioactive waste storage and core retention devices is somewhat related and so will be discussed briefly. In both of these areas, the substrate does not release any gas during the interaction. Here the concern is melting of the substrate and subsequent penetration by the heated solid material.

Emerman and Turcote[31] noted that this problem is similar to a simple Stoke's flow problem of a sphere sinking through a viscous medium. Here the medium is molten substrate material that is continuously produced by heat transfer from the internally heated sphere. The authors treat the problem in a purely analytical fashion by solving the coupled steady-state energy and momentum equations for the molten layer ahead of the sphere. Conduction in the substrate is not considered. While their analysis is not strictly applicable for either a concrete substrate or the debris geometry in a reactor accident, the method they used should also apply in the problem of interest.

Turland, et al[32] developed models for the penetration through core retention material by core debris. Again, since the substrate was not gas-releasing, only melting was considered. The primary contribution of this work was the development of an efficient numerical method for calculating transient conduction in the unmelted substrate. In their isotherm migration method (IMM) they calculate the time-dependent position of specified isotherms rather than temperature as a function of position and time. This method may be very useful in the analysis of conduction in a concrete basemat since large changes in composition and thermal properties occur in the concrete when specified decomposition temperatures are reached.

Another limiting case which has been examined by Ahmed and Dhir[18] is that in which the substrate is gas-releasing but does not melt. Their model was based on observations of heated copper blocks penetrating a subliming dry ice substrate. Although their final result was a convective heat transfer coefficient which was correlated to their experimental results, the form for the correlation was based on a solution of the momentum and energy equations for the gas film. By applying their analysis to the problem of a melting and gas-releasing concrete basemat, it may be possible to use their correlation by simply replacing gas properties by properties for the two-phase mixture of molten concrete and released gas. However, without some experimental verification such an extrapolation would be of questionable validity.

There have been very few attempts at detailed modeling of hot solid core debris interactions with concrete. The work that has been done varies from a detailed treatment of an isolated aspect of the interaction such as conduction in the concrete and water migration to rough scoping calculations which attempt to determine which phenomena are of the greatest importance. Both types of modeling are useful as preliminary steps to the development of more complete models.

The USINT computer code[33] was developed at Sandia to examine concrete response to the high heat fluxes which might be encountered in reactor accidents. It requires user-specified heat fluxes as input and calculates heatup of the concrete and subsequent gas release. It makes no attempt to calculate ablation of the concrete surface. Although this restriction limits its usefulness in core-concrete interaction calculations, the physical models employed in USINT represent the most complete treatment of concrete thermal response currently available. For this reason USINT will provide a benchmark for any hot solid model developed in connection with the Hot Solid tests.

Corradini[34] has derived a somewhat less detailed model for concrete response which does include ablation. In order to facilitate an analytical solution, he assumed that the thermophysical properties of concrete are constant and that any melted concrete is instantaneously removed from the surface. While the latter may be a reasonable approximation depending on the configuration of the debris, the properties of concrete are known to vary greatly with temperature. Average values were used in the analysis.

By assuming a polynomial dependence in position for the temperature profile (usually quadratic), the energy equation was integrated between the heated surface of the concrete at $x = 0$ and the thermal penetration depth, $x = \delta$. Here δ is the distance into the concrete beyond which no heat is conducted. Solving the resulting differential equation for $\delta(t)$ and then substituting back into the surface energy balance yields the concrete ablation velocity. Then assuming that H_2O and CO_2 are released from the concrete when specific decomposition temperatures are reached, time-dependent release rates can be determined from the calculated temperature profiles.

Using this model, Corradini examined the thermal response of concrete subjected to several different constant heat fluxes. He found that steady state ablation, which is assumed in computer codes such as CORCON-MOD1 and WECHSL, occurs only after a sometimes lengthy transient ablation period and that this transient period becomes longer as the incident heat flux is reduced. For the low heat fluxes associated with hot solid- concrete interactions, transient conduction in the concrete must be considered.

In an earlier analysis by Corradini[35] stratified debris layers that had solidified were examined. A metallic layer was on the bottom while the top layer was composed of mixed oxides. The two layers were treated using lumped-parameter properties. Energy was generated in the debris by decay of fission products while it was lost in the upward direction by radiation and natural convection and in the downward and sideward direction by conduction through a two-phase gas and concrete slag layer. The sidewalls were assumed to have receded far enough from the debris that ablation had ceased. Hence, the penetration of the concrete was only in the downward direction. The net energy available for ablation was reduced by the amount of the heat conducted into the concrete, which was calculated by a simple 1-D semi-infinite slab equation.

The primary conclusion from this simplified analysis was that the heat losses from the debris were small enough (1-2 MW) that it would remain at least partially molten for a considerable length of time--on the order of weeks or months depending on fission product retention in the debris and its geometry. Regardless of the accuracy of this conclusion, it does emphasize the need for understanding the transition between molten and solid debris behavior.

B.3. Transition Between Melt-Concrete and Hot Solid-Concrete Interactions

As just indicated, the transition between molten and solidified debris may extend over a lengthy period of time. Because of this, an understanding of this intermediate state is vital to an assessment of the safety aspects of core-concrete interactions. Currently, even the nature of the solidification process is not well-understood.

Two distinct mechanisms for solidification have been considered in the past. The core melt can be assumed to solidify in essentially a homogeneous fashion thus forming a solid/liquid slurry, or in the other limiting case, freezing of the melt may occur only at boundaries across which heat is transferred. In the former situation, the core-concrete interaction continues to be governed by convective heat transfer mechanisms (at least until the solid becomes the continuous phase) while in the latter, heat transfer at the core-concrete interface may be conduction-limited.

Solidification in a melt-concrete interaction is governed by two competing effects. Heat transfer at the melt boundaries tends to cause crust formation, while vigorous gas bubbling tends to break up any boundary crusts and mix the solid and liquid phases of the debris. In the limit of high gas flow, the debris would tend toward a slurry, while in the other limit of zero gas flow, a stable growing crust is more likely. Unfortunately,

little experimental or analytical work has been done to quantify the relative magnitudes of these effects or identify criteria for the transition between the two.

Previously discussed melt-concrete computer codes such as CORCON-MOD1 and WECHSL assume that the melt layers solidify in the form of a slurry. The same heat transfer mechanisms are assumed to be operative whether the core debris is molten or partially solidified. Unfortunately, because conduction-limited heat transfer is not included in these codes they are no longer valid when one or both of the debris layers is solid. This sometimes limits their applicability to only the first few hours of the core-concrete interaction.

Recently developed computer codes, CORCON-MOD2[36] and DECOMP[37] assume that stable crusts can form at the boundaries of the melt. The thickness of the crust is then governed by an energy balance at the boundary. While both codes attempt to model essentially the same phenomena, there are significant differences in the assumptions and approximations they employ. The following discussion outlines some of the important modeling features of each. It should be noted that CORCON-MOD2 is still evolving; the models discussed here represent those that have been reported prior to this writing.

In creating CORCON-MOD2, the crust formation model was added to CORCON-MOD1 in such a way that the number of basic changes to the code were minimized. Heat transfer between the internal melt pool and the crust is calculated using the same convective heat transfer correlations used in MOD1. A stable gas film is still assumed to exist between the core debris and the concrete, with heat transfer through the film being a combination of convection and radiation. Because the heat flux through the bottom and top surfaces are radially uniform, the crusts at those surfaces are of uniform thickness. Crusts at the radial boundaries of the melt, on the other hand, are assumed to have uniform crusts only within a melt layer. Area-averaged oxidic and metallic layer heat fluxes are used in the crust thickness calculation.

Cole[36] has reported the results of a sample accident calculation using CORCON-MOD2. Comparison calculations were run with and without the crust formation model included. The only significant difference between the two results was in the cavity erosion pattern. Here crust formation in the metallic layer adjacent to the concrete provided an additional thermal resistance which resulted in reduced heat transfer and concrete erosion. In the oxidic layer, a crust formed only at the top surface. This led to reduced radiation heat loss, higher layer temperatures, and greater heat transfer to the concrete. In terms of volume of concrete eroded and amount of gas released, however, the results for the two calculations were almost identical. As Cole concluded, this indicates the extent to which the CORCON calculation is governed by conservation of energy.

DECOMP[37] was developed as part of the MAAP program for the Industry Degraded Core Rulemaking Program (IDCOR). Like CORCON-MOD2, DECOMP assumes that heat transfer between the melt and the crust is governed by convection. (It is not clear from Ref. 37 whether the convective heat transfer coefficient, h, is parametrically input to the code or calculated using heat transfer correlations.) However, unlike CORCON, DECOMP assumes that the melt is a homogeneous mixture of metals and oxides and that this mixture is circulated uniformly within the debris crust. As a result, heat transfer and crust growth are also assumed to be constant at the core-concrete interface. Since upward heat transfer is controlled by a different mechanism (radiation and/or surface boiling) growth of the top surface crust is calculated separately.

In calculating heat transfer to the concrete, DECOMP assumes direct contact between the debris and the concrete surface--there is no gas or two-phase film separating the two. Hence the external crust surface is the same temperature as the concrete surface. When the concrete is ablating, this temperature is just the assumed ablation temperature. During ablation, the parabolic temperature profile in the crust is given by (as is also the case in CORCON-MOD2):

$$\frac{T - T_a}{T_m - T_a} = 1 - \left[\frac{x}{x_c}\right]^2$$

This equation has one unknown; the crust thickness, x_c. Here T_m is the melting temperature of the crust, and T_a is the concrete ablation temperature. The crust thickness is then found by solving the following differential equation which is based on an energy balance for the crust:

$$\frac{dx_c}{dt} = -\left[\frac{h(T_F - T_m) + Qx_c + \frac{2k_F(T_m - T_a)}{x_c}}{\rho_f L_f}\right]$$

Here the first term in the numerator of the right hand side represents convection to the crust from the melt, the second term accounts for internal heat generation, and the last term is the heat conducted to the concrete. The denominator of the right hand side represents the volumetric latent heat of fusion (J/m^3) for the material mixture comprising the crust.

Once the crust thickness is calculated, heat conduction to the concrete is simply given by the third term in the numerator of the above equation. As in CORCON, this heat flux is then substituted into the steady state ablation equation to give the concrete ablation rate.

Since DECOMP assumes that heat transfer rates are the same in the downward and radial directions, the concrete cavity erodes uniformly. This assumption is contradicted by the current body of experimental data, where in most cases axial erosion is significantly greater than radial erosion. This is especially true for experiments in which the debris remains solid throughout the test.[19,21] Because the debris surfaces are rigid, a growing two-phase (molten concrete and released gas) film forms between the debris and the uneroded cavity sidewalls. The additional thermal resistance provided by this film reduces the erosion rate and may eventually cause it to stop.

By considering crust formation and the resulting conduction-limited heat transfer, CORCON-MOD2 and DECOMP theoretically can calculate both the initial melt-concrete and the subsequent hot solid-concrete interactions. However, even assuming that crust formation is the correct transition mechanism, there may be enough significant differences in behavior for the two types of core-concrete interactions to warrant a more individualized treatment. Aside from previously discussed differences in sidewall erosion, there should be little or no mixing of newly eroded concrete with the rest of the debris. Instead, this molten concrete will probably be pushed to the top of the debris where it will form a growing crust. While CORCON does predict a top oxide layer, its top layer is a mixture of core and concrete oxides and is thus internally heated. A concrete slag crust, on the other hand, has essentially no internal heating and therefore provides a more effective insulating barrier to upward heat transfer. As mentioned earlier in the discussion of the FRAG tests[21] this is especially important in the consideration of coolant addition as a possible accident mitigation feature.

B.4. Other Models

In addition to these models for core-concrete interactions, other models have been proposed in a related area: sodium-concrete interactions.[38,39] This work has been done to assess the safety of Liquid Metal Fast Breeder Reactors. For reasons that will soon become apparent, only the model in Ref. 38 will be discussed here.

The SLAM computer code[38] has recently been developed at Sandia National Laboratories (SNLA) by Suo-Anttila. Many of its models have been tested and verified by comparison to results of experiments conducted at SNLA and elsewhere. While sodium-concrete interactions are generally quite different than core-concrete interactions, there are several similarities.

Sodium-concrete interactions are controlled by the rate of the exothermic chemical reactions between the liquid sodium and concrete constituents. Because the bulk sodium temperature is always less than the melting temperature of the concrete,

ablation occurs as the result of chemical reactions or dissolution of the concrete (primarily $CaCO_3$) by the sodium pool rather than by melting. These phenomena are obviously very different from what has been described for the interaction of internally heated core debris (especially in solid form) and concrete. What is the same, however, is the thermal response of the concrete to an imposed heat flux. When heated the subsurface concrete behaves the same whether the heat flux is produced by chemical reactions or a combination of conduction, convection, and radiation heat transfer.

Of the models discussed in this section, the only comparable treatment of concrete response is found in the USINT computer code.[33] However, the solution techniques employed in SLAM are simpler and should be computationally more efficient. SLAM has the added benefit of being able to handle concrete ablation and the resulting calculational complexities associated with a moving interface. For this reason, SLAM will be used as the foundation for the hot solid-concrete model which will be developed in conjunction with the proposed experiments.

For a more detailed discussion of SLAM and the additional features to be incorporated into the hot solid model, see Section V.

B.5 Modeling Summary

The models discussed in the preceding sections cover the entire range of core-concrete interactions from the initial molten debris phase to the final phase where the debris is completely solidified. Unfortunately, the available models are vastly different from one another, and there is insufficient experimental data available to allow one to make an educated decision about which is the most accurate. In fact, it is unlikely that any of the models treat all of the important phenomena correctly.

The uncertainties involved in the melt-concrete interaction that most affect the hot solid phase include the degree of mixing between the oxidic and metallic materials in the debris and the mode of transition between molten and solid debris. If gross mixing is assumed, the properties of the solidified mixture will be quite different from those of stratified debris. The property that most effects heat transfer in the conduction-limited process is thermal conductivity. Since thermal conductivity for the metallic and oxidic phases are at least an order of magnitude different from one another, this single uncertainty may govern the problem. Further, if the debris is stratified the concentration of decay heat sources will be much greater in the oxidic layer. When this is true the metallic layer may solidify while the oxidic layer remains molten. Hence, concurrent hot solid-concrete and melt-concrete interaction would be taking place.

The transition from molten to solid debris can occur via two mechanisms: formation of either a homogeneous solid/liquid slurry or boundary crusts. In the former, heat transfer at the core-concrete interface is still controlled by convection, while in the latter heat transfer is conduction limited. These two heat transfer processes are sufficiently different that the timing of the transition to solidified debris will be affected. While the crust formation mechanism allows a smoother transition to hot solid behavior, it is not clear that a stable crust will form at boundaries across which there is significant gas flow.

As indicated previously, the cause of this modeling uncertainty is the current lack of prototypic experimental results. In the Hot Solids program analytical and experimental efforts are closely coupled. Models are being developed and modified according to what is observed and measured in the tests. By doing this, the uncertainty associated with other core-concrete models can be reduced.

III. EXPERIMENTAL RESULTS

Two preliminary experiments, HSS-1 and HSS-3, were performed in order to measure, model, and assess hot solid core-concrete interactions. These experiments measured erosion and thermal response but did not measure gas evolution, water release, or aerosol production. The HSS-1 experiment ablated 6 cm of limestone-common sand concrete in a little more than three hours using a 9 kg slug of 304 stainless steel at an average debris temperature of 1350°C. The HSS-3 experiment ablated 6.5 cm of limestone-common sand concrete in four hours using a 10 kg slug of 80% UO_2-20% ZrO_2 and an average debris temperature of 1650°C. Details and data from these tests are presented in the following sections. An overall comparison of the two tests is given in Table II.

A. Hot Solid Stainless Steel/Concrete Interaction Experiment (HSS-1)

As part of the Hot Solid Program, the HSS-1 experiment was designed as a scoping test to achieve three goals: (1) develop and test a one-dimensional crucible design for future 10 kg Hot Solids Tests, (2) determine the limits and capabilities of real time Co^{60} X-ray imaging techniques for measuring concrete erosion rates, defining debris-concrete interaction mechanisms, and observing overlying crust formation and, (3) obtain preliminary hot-solid/concrete temperature data in order to develop and test thermal conduction models for limestone common sand (LCS) concrete and the 1-D crucible design.

The HSS-1 experiment (Figure 1) stood thirteen inches high and eight inches in diameter and used a 9 kg 304 stainless steel slug to simulate hot solid attack. This slug was six inches in diameter and three inches high and was inductively heated over

limestone common sand (LCS) concrete in a seven inch diameter insulated alumina sleeve to approximate 1-D (axial) basemat erosion. Instrumentation consisted of both real time x-ray imaging and on-line video recordings to measure basemat erosion and crust growth as well as a matrix of 34 S and K-type thermocouples to define the associated radial and axial temperature profiles. The insulated sleeve configuration was positioned in a 13-turn, 8-1/2 inch diameter induction coil and was powered by a 50 kw 3000 Hz motor generator set. A ZrO_2 coverplate was used to reduce radiation losses from the slug and one side of the plate was tilted at a 45° angle to provide an optical viewing port for the video camera. The HSS-1 test was run in open air at atmospheric pressure and at an ambient temperature of 10°C.

Power to the induction coil was initially set at 10 kw. After one hour, thermocouples within the steel slug reached temperatures of 1350-1400°C and power was reduced to 8 kw in order to maintain concrete erosion temperatures without exceeding the 1450°C melting point of 304 stainless steel. Erosion of the LCS concrete began at around 70 minutes and continued slowly for three more hours (see Figure 2). The erosion was asymmetric at onset, becoming roughly axisymmetric after 90 minutes. After one hour of erosion, a film of molten concrete slowly formed over the top of the slug. This film began to cool and formed a more solid crust after two hours of erosion. After nearly three hours of erosion, the stainless steel slug began to show signs of localized melting. This continued for ten or fifteen additional minutes at which time (four hours after start-up and three hours after erosion started) the entire slug was obviously completely molten. Power to the coil was turned off at this point and the test was terminated.

Posttest disassembly of the HSS-1 package showed that the insulated alumina sleeve had sustained a number of hairline cracks at and above the hot solid/concrete interface. Review of the video films confirmed that these cracks occurred early during the first hour of the test and did not seem to propagate after erosion had begun. Disassembly also showed that the slug had been molten, that an overlying crust had formed which was relatively dense material laced with gas pockets, and that the molten steel/concrete interface was flat and uniform across the diameter of the alumina sleeve. These observations also correlate with the video tape and x-ray imaging data. Although the alumina sleeve was cracked, neither molten concrete nor steel completely penetrated those cracks and neither material interacted with or eroded the sleeve wall at any point.

Posttest analysis of the thermocouple data (Figure 3 and Appendix B) showed general agreement with the erosion data (Figure 4) and the heat conduction analysis. The 9 kg slug of 304 stainless steel showed an initial temperature rise of 700°C in twenty minutes. These data coincide with pretest calorimetry data which indicate that roughly 40% ($\pm$5%) of the induction coil power is transferred to a similar 8.6 kg slug independent of

Table II

UO_2 vs Steel Hot Solid Interactions

	HSS-1	HSS-3
Debris	9 kg 304 SSteel	10 kg UO_2-ZrO_2
Slug Size	14 cm x 8 cm	13 cm x 18 cm
Erosion	6 cm	5.5 cm
Avg. Losses	4.9 w/cm^2	3.6 w/cm^2
Erosion Rate	2.0 cm/hr	1.5 cm/hr
Avg. Power	3.2 kw	3.6 kw
Crust Type	Overlying	Underlying

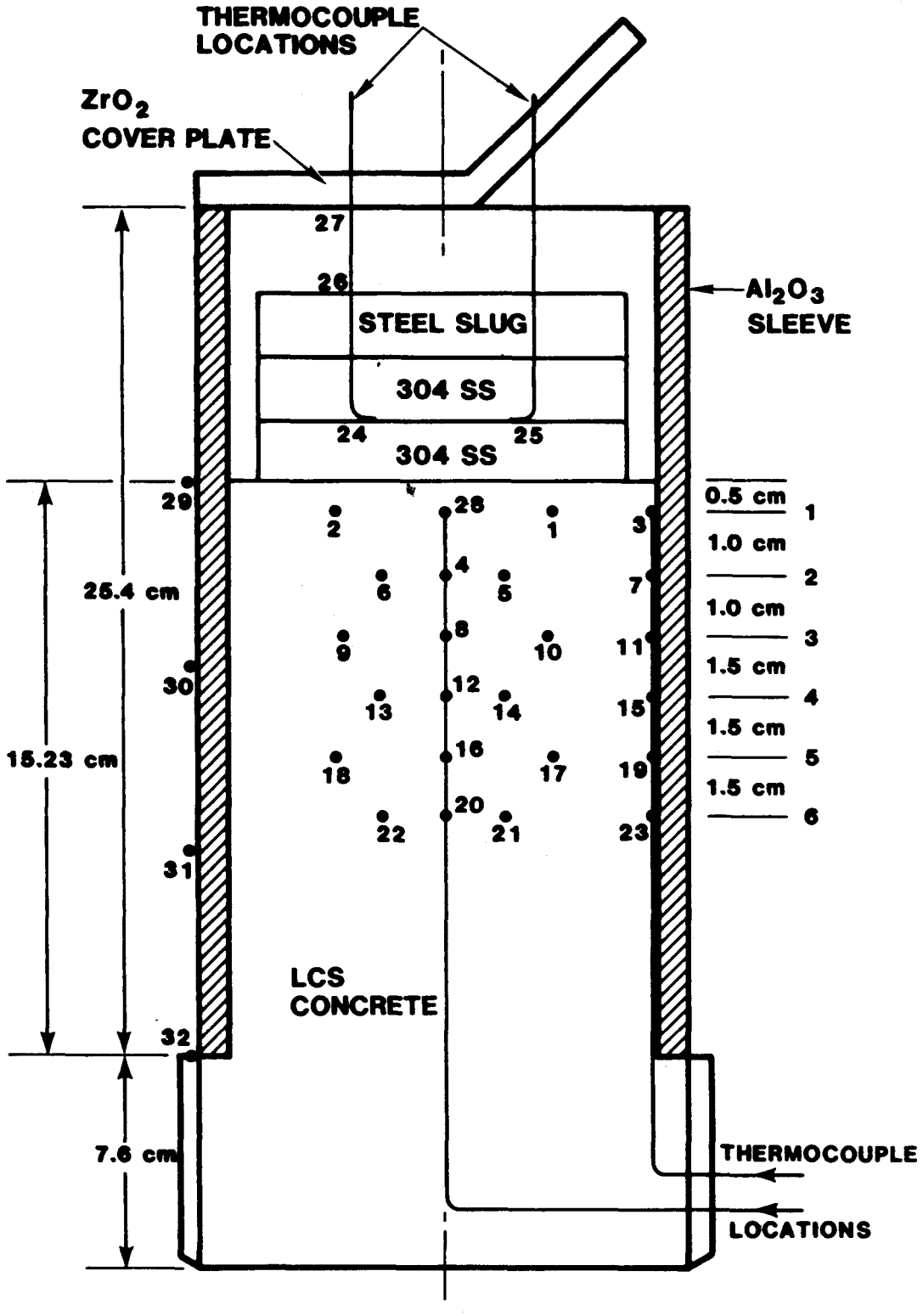

Figure 1. HSS-1 Geometry

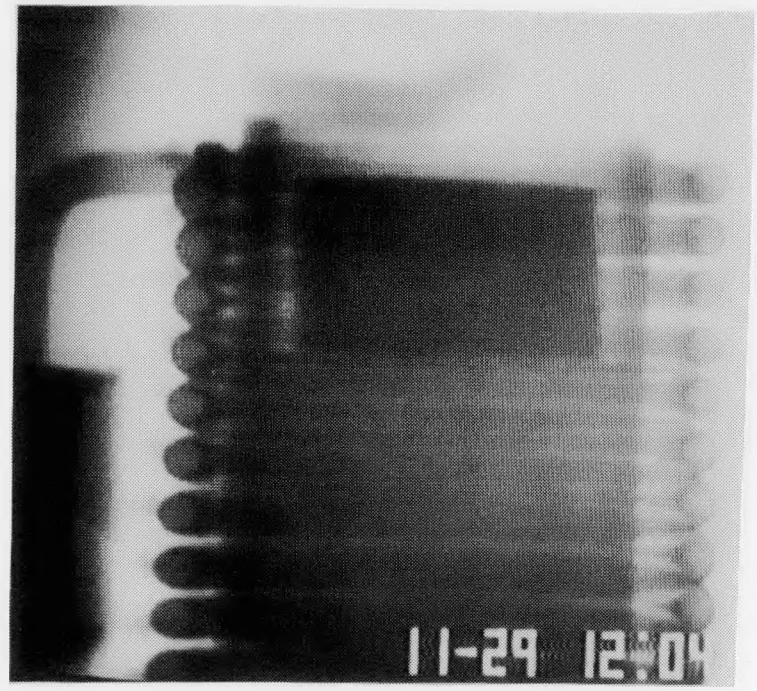

a. Initial condition with no crust or erosion

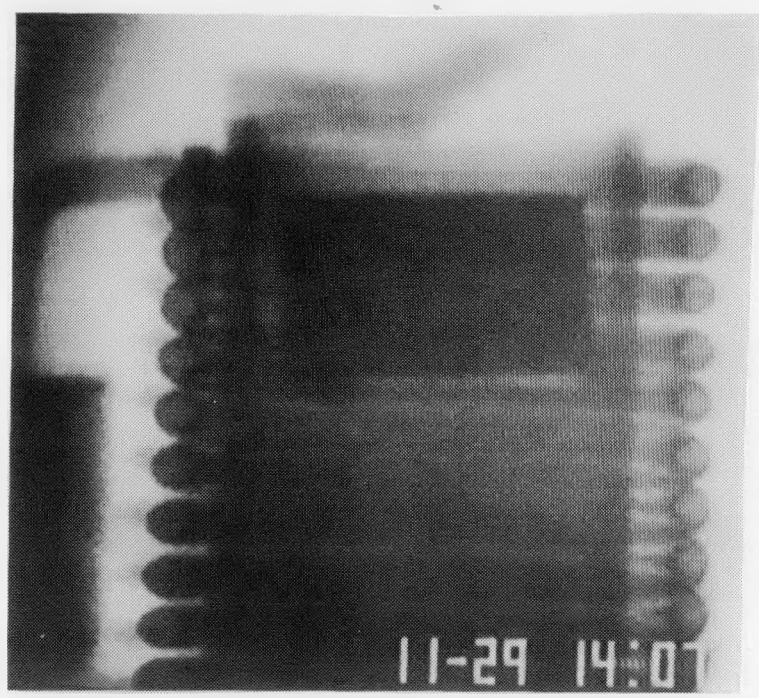

b. Asymmetric erosion without crust (t = 2 hr)

Figure 2. HSS-1 X-Ray Imaging Data

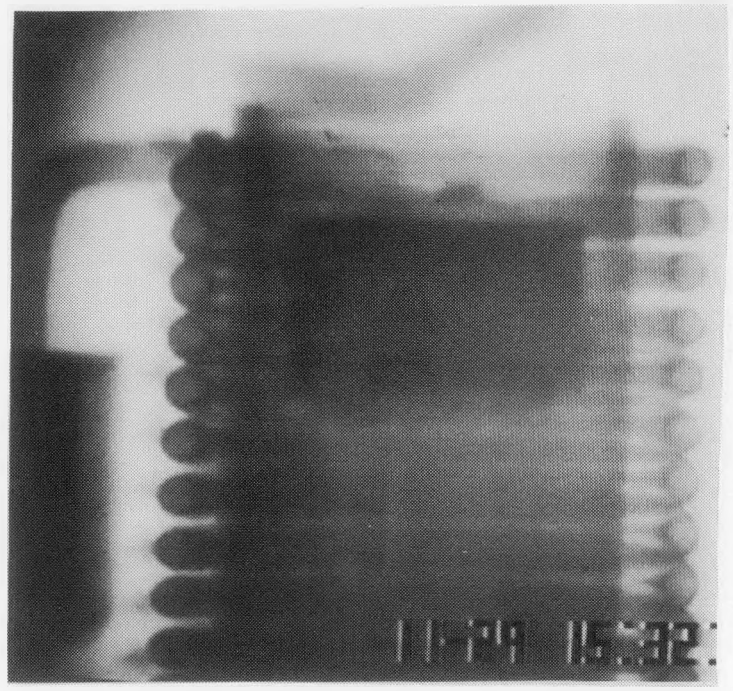

c. Axisymmetric erosion with crust (t = 3.5 hr)

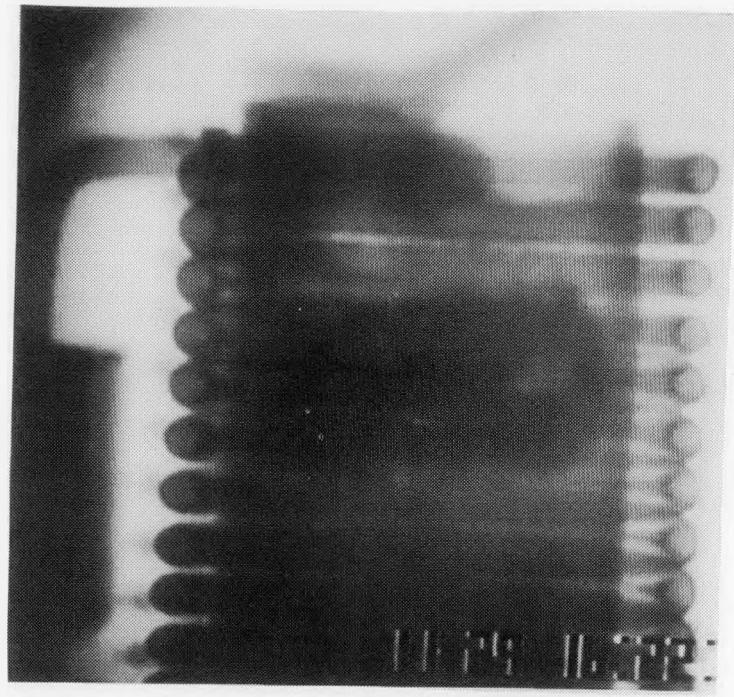

d. Molten attack (t = 4.2 hr)

Figure 2. HSS-1 X-Ray Imaging Data (Continued)

power level for centerline coil positions at temperatures between 400°C and 1200°C. The 9 kg 314 stainless steel slug used on HSS-1 eroded 6 cm of limestone-common sand concrete in three hours at an average debris temperature of 1350°C. The rate of erosion was fairly constant throughout the course of the erosion with a slight increase when the steel slug began to melt.

On the whole, the HSS-1 experiment was successful in producing and recording the axial penetration of hot solid material through a concrete basemat. Several design modifications are indicated, however, before attempting a fully instrumented Hot Solid test.

The crucible design used in HSS-1 was successful in achieving a 1-D axial erosion pattern without sidewall attack. Future designs, however, will require additional containment when water vapor and gas samples are taken. One proposed design improvement will be to use a high temperature ceramic sleeve in addition to the alumina sleeve. The ceramic sleeve will provide additional containment and can also be isolated from the rest of the configuration to eliminate significant thermal gradients which are believed to be the principal cause for cracking within the alumina.

The real time ^{60}Co x-ray imaging technique used in HSS-1 was outstanding in every respect. Both symmetric and asymmetric erosion patterns were observed with resolutions as high as 1 mm/sec. Crust formation, energetic gas generation, and melt/concrete interactions were also observed in great detail. This technique has proved to be much better than expected and is now ready for use in the remainder of the Hot Solid Program.

Other design improvements for the Hot Solid configuration include the use of a mild steel slug to provide an additional 100 K margin between the ablation temperature of concrete and the melting point of the hot solid simulant and the use of a complete zirconia insulator cap on the slug to reduce early time asymmetric erosion.

B. Hot Solid UO_2/Concrete Interaction Experiment (HSS-3)

The HSS-3 experiment was also designed as a scoping test. The main objectives for HSS-3 were to determine whether or not the geometry and diagnostics developed in the steel/concrete interaction experiments could be applied to an experiment using UO_2 as the slug material.

HSS-3 used a 10 kg slug of 80% UO_2-20% ZrO_2 to simulate hot solid attack. This slug was inductively heated using five embedded tungsten rings (1.0 cm o.d. - 5 cm i.d. - 0.3 cm thick) spaced 3 cm apart. The UO_2 slug stood 18 cm high and 13 cm in

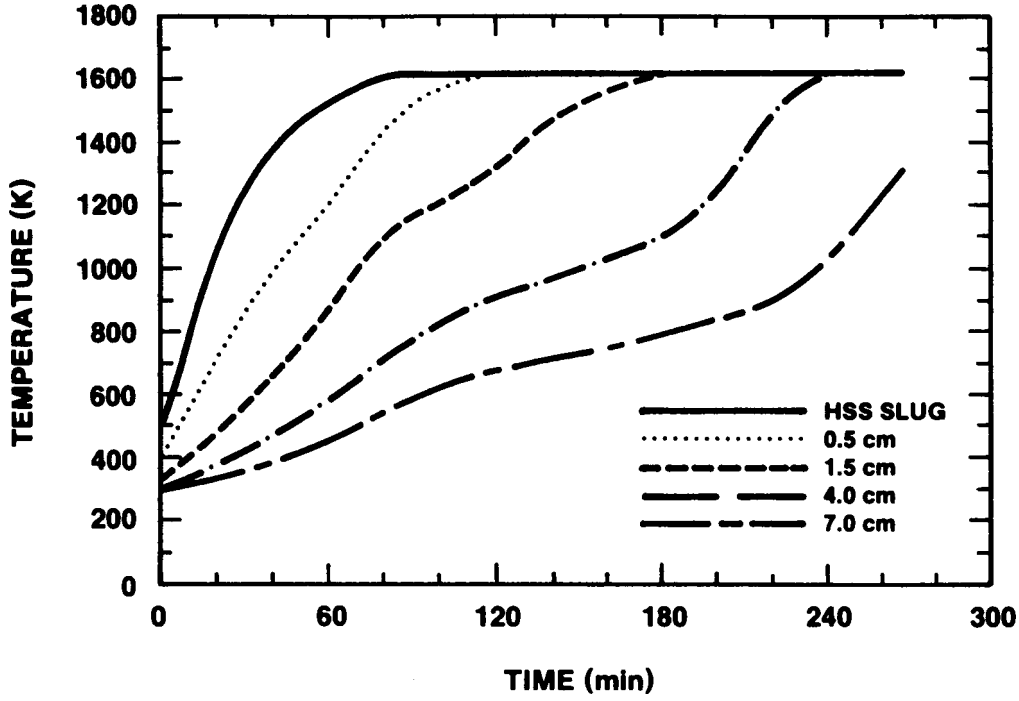

Figure 3. HSS-1 Composite Thermal Profile

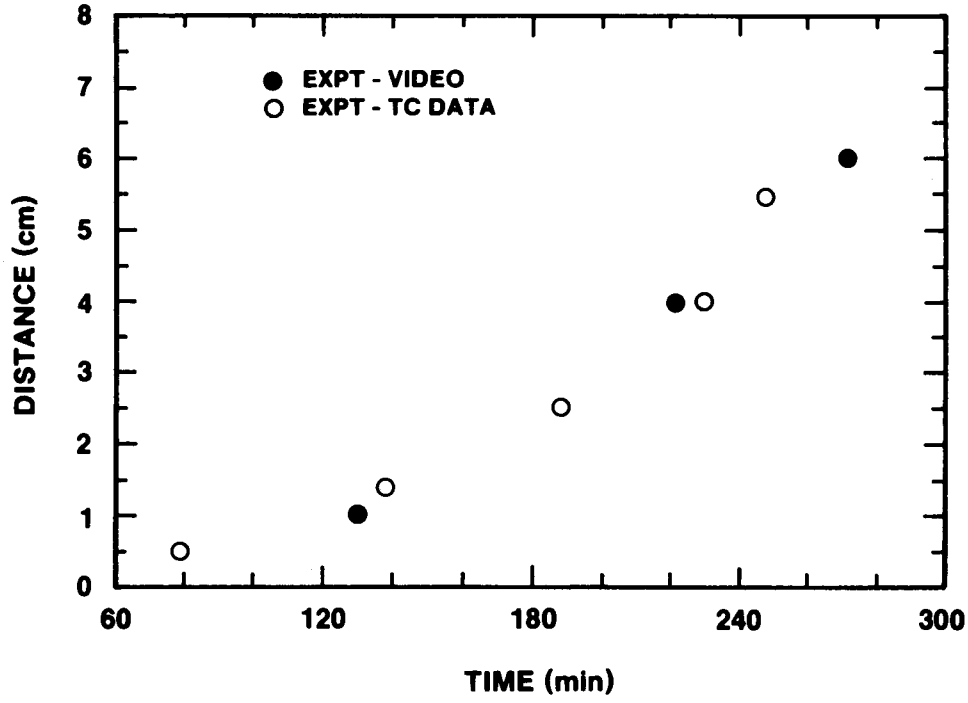

Figure 4. HSS-1 Erosion Distance Profile

diameter and was instrumented with C and S type thermocouples. All other aspects of the experimental configuration were exactly as in HSS-1.

Power to the induction coil (Figure 6) was applied more gradually in HSS-3 than in HSS-1. After three hours, erosion began when the interface temperature reached 1300°C. Erosion continued at an approximately constant rate for four more hours. Unlike HSS-1, ablation was symmetric at all times and was not accompanied by substantial crust growth or formation. After four hours the erosion front reached the practical limit for measuring thermocouple responses and the test was terminated.

Posttest disassembly of the HSS-3 package showed that both the UO_2 slug and the alumina sleeve had remained essentially intact during the test. Hairline cracks appeared in both structures, however, and the embedded rings in the UO_2 slug were exposed to the atmosphere. An underlying crust composed of grey UO_2/concrete slag material filled the gap between the UO_2 slug and the alumina sleeve for a height of 2 to 3 cm above the original concrete interface. These observations correlate with the x-ray imaging data.

Analysis of the thermocouple data (Figure 6 and Appendix B) again showed general agreement with the x-ray erosion data (Figure 7. These data confirmed that the tungsten ring assembly was able to absorb roughly 75% of the power applied to the induction coil.[40] The 10 kg slug of 80% UO_2-20% ZrO_2 ablated 5.5 cm of limestone-common sand concrete in approximately four hours at an average debris temperature of 1650°C. Once again the rate of erosion was fairly constant throughout the course of the HSS-3 experiment.

The HSS-3 experiment was successful in producing and recording the axial penetration of hot solid UO_2 through a concrete basemat material. As with HSS-1, however, several design changes are indicated before a fully instrumented hot solids test can be run. Additional containment to facilitate measurements of water vapor and gas evolution is the first priority improvement and should be accomplished with the addition of a second ceramic sleeve outside of the alumina sleeve now employed. Once the design changes suggested from the results of HSS-1 and HSS-3 have been made, fully instrumented tests will be run using both steel and UO_2 for solid attack.

IV. ANALYSIS

A. Current Hot Solid Modeling Efforts

A hot solid-concrete interaction model, HOTROX, is currently being developed at Sandia as part of the Hot Solid test program. The foundation of the present model is the SLAM computer code[32] which was developed in the area of sodium-concrete interactions.

While sodium-concrete interactions are generally quite different from core-concrete interactions, there are several similarities. In the following discussion of the HOTROX model, changes made to SLAM will be outlined.

What drives the sodium-concrete interaction is the rate of chemical reaction between the sodium and the constituents of the concrete. The resulting exothermic reaction supplies heat which is then conducted into the concrete. These reactions also dissolve the concrete at the interface. While the ablation mechanism and heat source are fundamentally different in a core-concrete interaction, the thermal response of the concrete to a given heat flux will be the same. The transient conduction models in SLAM have therefore been incorporated directly into HOTROX.

As mentioned before, SLAM is a one-dimensional model; conduction and ablation take place along the axial coordinate direction. The Hot Solid tests are specifically designed to isolate concrete response in the axial direction, thus the SLAM 1-D model is ideally suited for Hot Solid test analysis.

The primary modification made to SLAM was to its treatment of the sodium/hot solid region. Here the chemical reaction and mass diffusion models in SLAM were replaced by a 1-D heat conduction model that includes internal heat generation. At the interface with the concrete, temperature and conduction heat transfer are assumed to be continuous. At the opposite surface of the solid, heat is transferred by combined convection and radiation.

Although HOTROX explicitly considers only one-dimensional heat transfer, heat losses in other directions (i.e., through the crucible sidewalls) can be included by modifying the user-specified input power. This, of course, requires that these losses be either calculable or measured directly during the experiments. For example, given the response of sidewall thermocouples, the sidewall heat flux can be "backed out" by performing an Inverse Heat Flux calculation. The solution technique proposed by Beck[33] is ideal for this.

B. Analysis of the Hot Solid Experiments:

The HOTROX model has been applied to analysis of the HSS experiments.

In the following discussion, experimental and calculated results are compared. Two points of comparison have been chosen for this: concrete erosion and concrete thermal response. These two have been chosen for two fairly obvious reasons. First, experimental data are readily available, and second, concrete erosion and thermal response drive all other phenomena from core-concrete interactions. The former affects basemat penetration time, while the latter controls gas release and hence, flammable gas production.

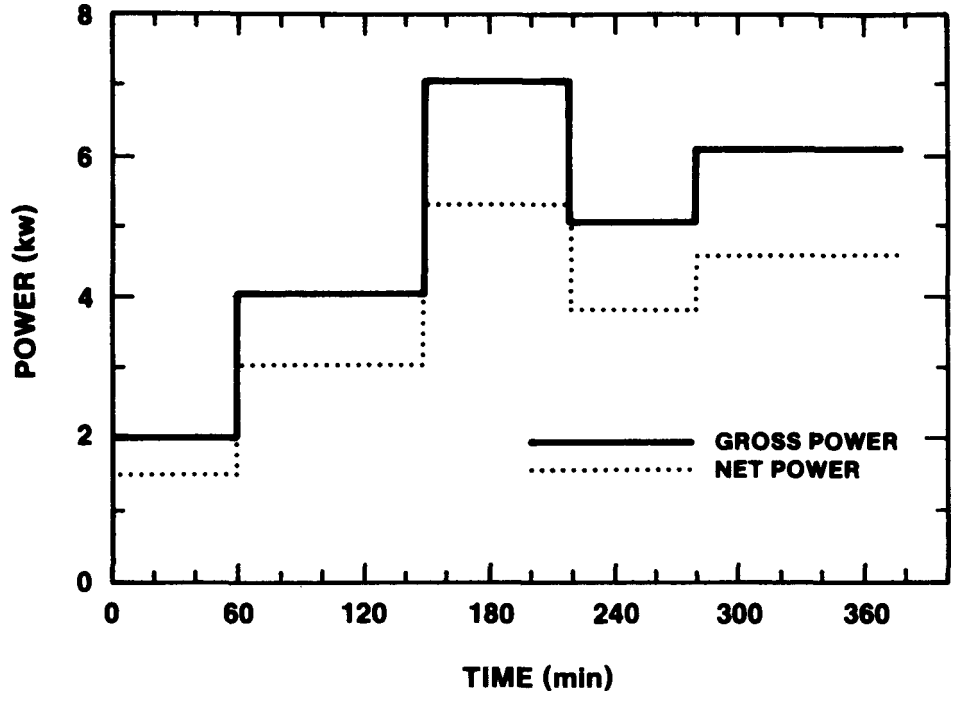

Figure 5. HSS-3 Power History

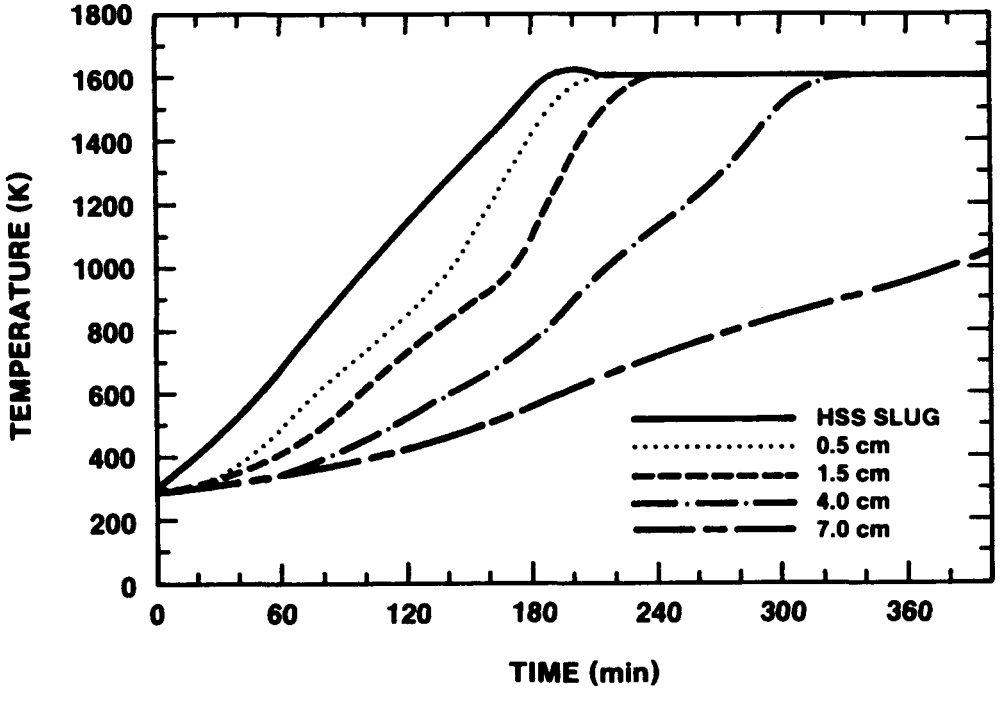

Figure 6. HSS-3 Thermal Profile

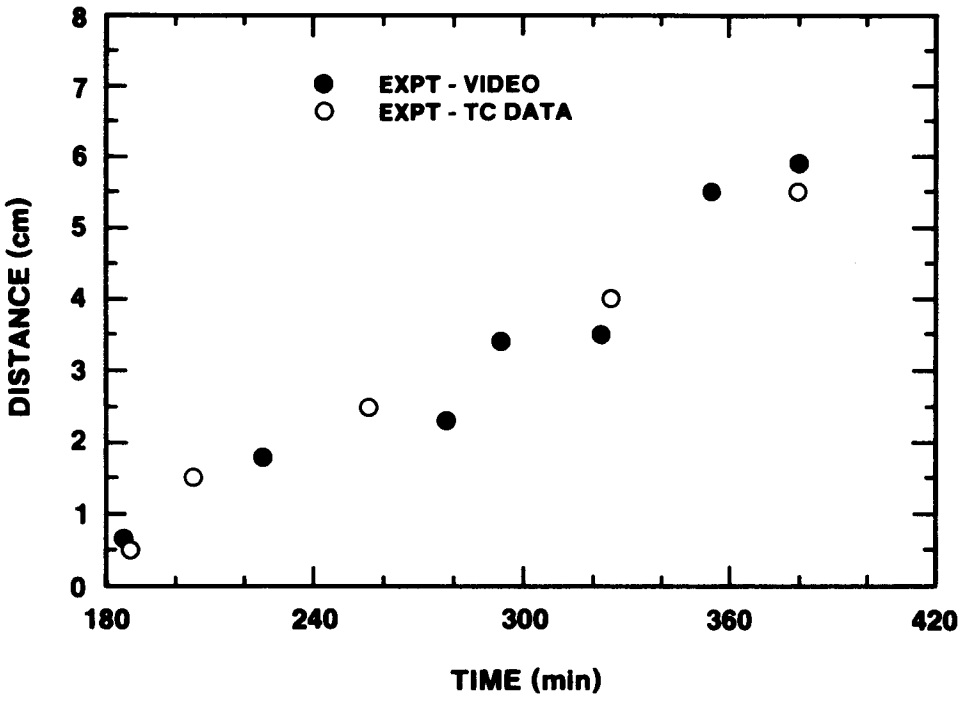

Figure 7. HSS-3 Erosion Distance

HOTROX requires that the user specify, among other things, the internal power supplied to the slug and the emissivity of the top surface of the slug. Other user inputs are given in Appendix C. The internal power is assumed to be uniformly distributed. (A future version of HOTROX will allow nonuniform heating, e.g., the imbedded tungsten rings in HSS-3.) This is a reasonable assumption for the slug in HSS-1 since the high thermal conductivity of the steel minimizes the effects of the inherently nonuniform heating of the induction technique.[40]

Radiation heat transfer is treated very simply in the current version of HOTROX. The top surface of the slug is assumed to radiate with a constant emissivity to a body which is at a constant, user-specified temperature. In the actual experiments, surrounding surfaces heat up thereby reducing radiant heat transfer. The analysis is further complicated by the geometry of the experiments. Because part of the top plate is tilted upward, the surface "sees" both a radiating surface and an open surface. To account for these effects, albeit in a very approximate manner, the effective emissivity of the slug surface was set to 0.4. This represents a significant reduction in typically assumed values for oxidized steel of 0.7 to 0.8.

The results of the HOTROX calculation for HSS-1 are presented in Figures 8 and 9. The agreement between the calculated and experimental results is in general quite good. In both cases, erosion begins at between 60 and 70 minutes after the start of the test, and total erosion during the 280 minute test is approximately 6 centimeters. The calculated erosion rate is approximately 2 cm/hr for most of the test, while the experimental rate appears to increase from an initial value of 1.2 to 1.5 cm/hr to a final value of 2.5 to 2.7 cm/hr. The measured and calculated thermocouple response for two thermocouples placed in the concrete is shown in Figure 8. Also plotted is the calculated temperature at the hot solid-concrete interface. Once again, the agreement is quite good.

The HOTROX calculations for HSS-3 are shown in Figures 10 and 11. The agreement between the calculated and experimental results is reasonable but not so good as the HSS-1 analysis. The HSS-3 erosion data (Figure 11) starts at 180 minutes and reaches 5.8 cm at 360 minutes. HOTROX predicts HSS-3 erosion to start at 180 minutes and reach 6.8 cm at 360 minutes. The thermocouple data and HOTROX thermal analysis is shown in Figure 10. Here the HOTROX analysis shows good agreement with experimental data at a depth of 4.0 cm into the concrete, but predicts higher temperatures at the interface than were experimentally observed.

By matching a) the start time for concrete erosion, b) the average erosion rate, and c) the concrete thermal response, HOTROX appears to be giving an accurate representation of the HSS experiments. There are, however, several models in HOTROX that were not tested by the experiments. For example, because gas and

water releases from the concrete were not measured in the experiment, these important aspects of the calculation were not checked. Future tests which measure gas flow and water release will be used to develop gas and aerosol models in HOTROX.

There are also several phenomena which were observed in the experiments but which are not presently modeled in HOTROX. For example, slag flow and eventual crusting on top of the hot slug is not considered although it could conceivably be an important factor in a long-term interaction. Also, production of flammable H_2 and CO is not modeled in the code although it was observed to be significant during the experiments. Additional models may be included as more experimental data becomes available.

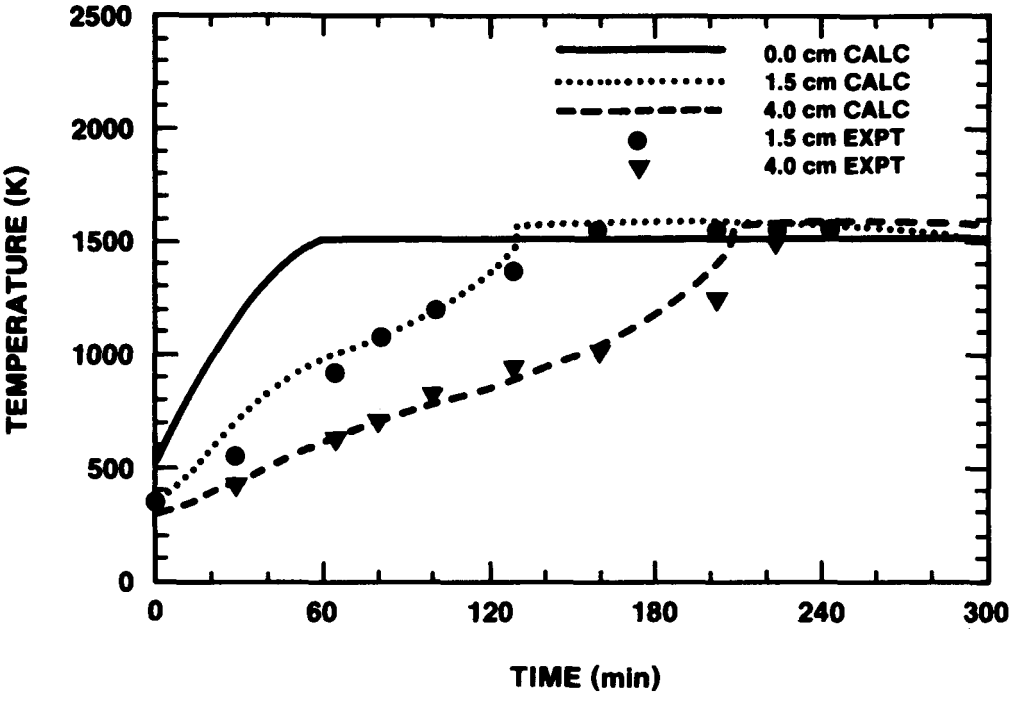

Figure 8. HSS-1 Thermocouple Temperatures

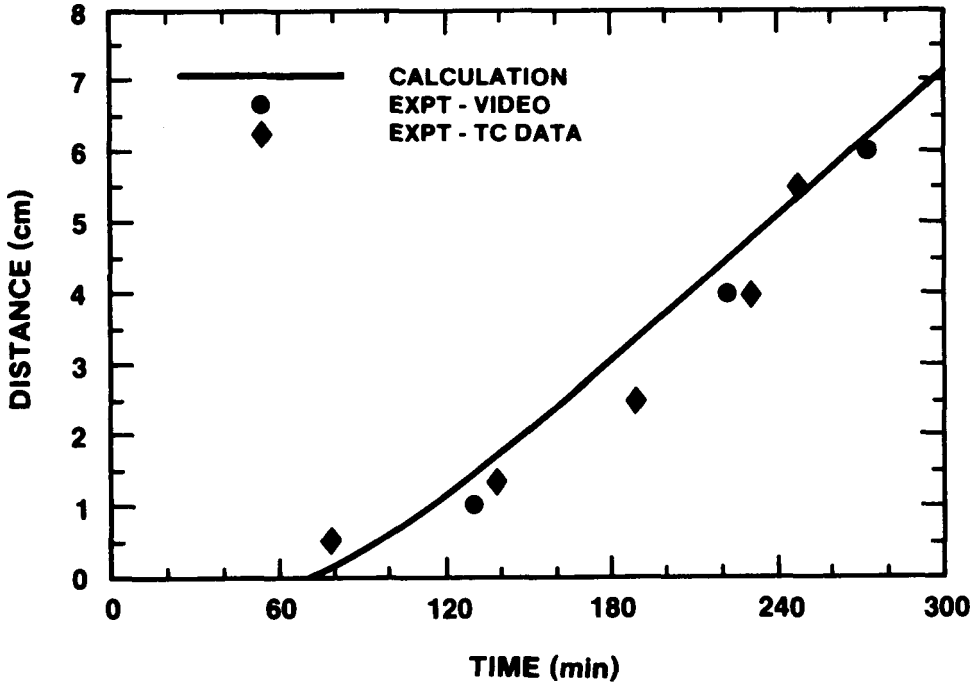

Figure 9. HSS-1 Erosion Distance

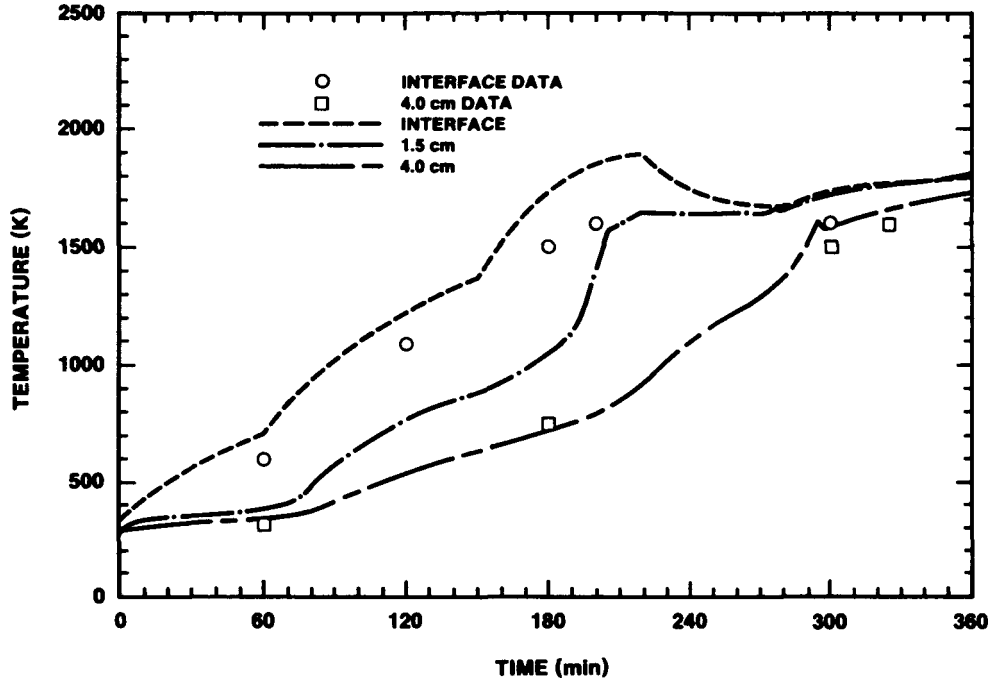

Figure 10. HSS-3 Thermocouple Temperature

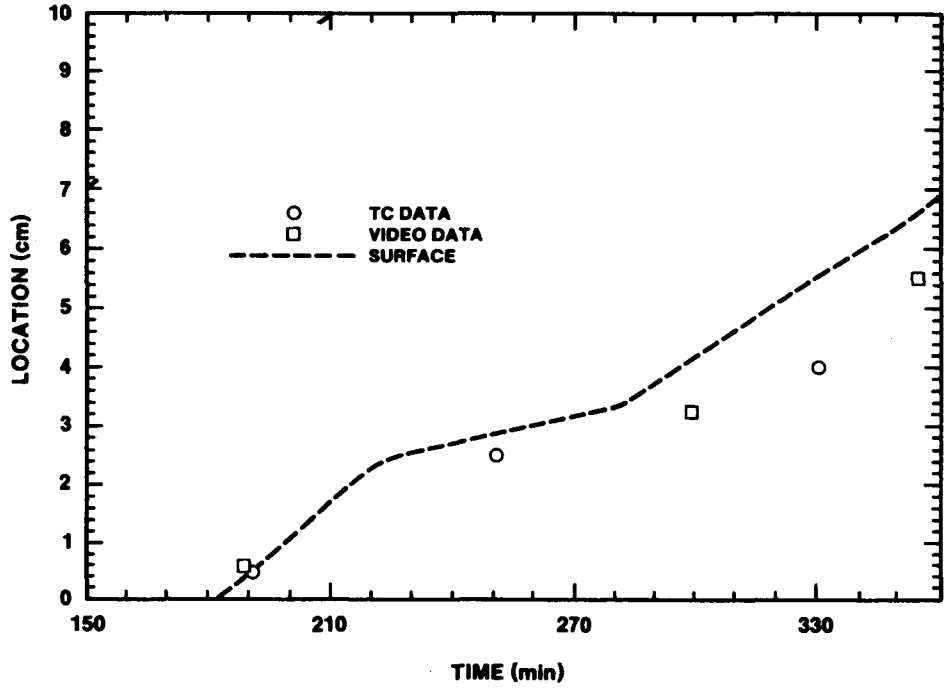

Figure 11. HSS-3 Front Locations

V. FUTURE WORK

The Hot Solids Program will be performed in three phases. Phase one will investigate interactions characteristic of highly conductive, medium density metallic core debris in contact with low conductivity, low density concrete. This work will be done using steel plate representing a monolithic slug over limestone common sand concrete. The objectives of this work will be to determine how debris configuration, power history, and geometry affect gas generation, heat flux partitioning, erosion, and crust formation. A separate post-test analysis will be done to determine the chemical and thermal properties of aerosols and crust materials.

Phase two of the program will investigate interactions characteristic of low conductivity, high density oxide core debris in contact with concrete. This will be done using first a solid UO_2-ZrO_2 monolith heated internally with tungsten rings and then fragmented UO_2-ZrO_2 heated with steel. These tests will provide additional information on the effects observed and modeled in Phase I as well as information on steel vs. UO_2 as a debris type and steel vs. tungsten as a heat source. These tests will also include post-test analysis to determine the thermal and chemical properties of crust materials and aerosols.

The computer model developed using these initial base case Hot Solid tests will be exercised, evaluated, and extended to reactor scale geometries. This will be done with Phase three experiments using larger geometries, different concrete types, and fragmented core debris. Together, these experiments will be used to exercise the base case 1-D model, to evaluate the effects of scaling up that model to intermediate and large scale safety analyses, and to expand the post-accident interaction phenomena data base.

Five tests are included in the initial effort. The first four tests will define the boundaries of a two dimensional interaction response surface whose variables are debris type and debris power history. The fifth test represents the mid-point of this statistical design space. Together these five tests along with any necessary replicates represent the first two phases of the Hot Solid Program and constitute a complete statistical design matrix which will be used to develop a one-dimensional (slab geometry), low temperature concrete erosion model. This model will also describe gas evolution, heat flux partitioning and fission product distributions as a function of debris power history aerosol.

References

1. USAEC, "An Assessment of Accident Risks in U.S. Commercial Nuclear Power Plants," WASH-1400, (August 1974).

2. "Core Meltdown Experimental Review," W. B. Murfin, editor, SAND74-0382, NUREG-0205, Sandia National Laboratories (March 1977).

3. D. E. Mitchell, M. L. Corradini, and W. W. Tarbell, "Intermediate Scale Steam Explosion Phenomenon: Experiments and Analysis," SAND81-0124, NUREG/CR-2145, Sandia National Laboratories (September 1981).

4. "Zion Probabalistic Safety Study," Commonwealth Edison Co., Chicago, IL (1982).

5. "Indian Point Probabalistic Safety Study," Consolidated Edison Co., Power Authority of the State of New York (1982).

6. C. Somerton, I. Catton, and L. Thompson, "An Experimental Investigation into Dryout in Deep Debris Beds," Tran. of the ASME (November 1981).

7. J. F. Muir, R. K. Cole, M. L. Corradini, and M. A. Ellis, "CORCON-MOD1: An Improved Model for Molten-Core/Concrete Interactions," SAND80-2415, NUREG/CR-2142, Sandia National Laboratories (July 1981).

8. G. A. Greene and C. E. Schwarz, "An Approximate Model for Calculating Heat Transfer Between Overlying Immiscible Liquid Layers with Bubble-Induced Liquid Entrainment," Proc. of the Fifth PAHR Info. Exhange Meeting, Karlsruhe, (July 1982) pp. 251-257.

9. "Light Water Reactor Safety Research Program Quarterly Report, Jan-March 1980," SAND80-1304/1 of 4, NUREG/CR-1509/1 of 4, Sandia National Laboratories (July 1980).

10. "Report of the Presidents Commission on the Accident at Three Mile Island - The Need for Change: The Legacy of TMI," J. G. Kemeny, Chrmn., Washington, D.C. (October 1979).

11. D. A. Powers and F. E. Arellano, "Large-Scale Transient Tests of the Interaction of Molten Steel with Concrete," SAND81-1753, NUREG/CR-2282, Sandia National Laboratories (January 1982).

12. D. A. Powers and F. E. Arellano, "Direct Observation of Melt Behavior During High Temperature Melt/Concrete Interactions," SAND81-1754, NUREG/CR-2283, Sandia National Laboratories (January 1982).

13. D. A. Powers, "Sustained Molten Steel/Concrete Interaction Tests," SAND77-1423, NUREG/CR-1066, Sandia National Laboratories (June 1978).

14. "Light Water Reactor Safety Research Program Quarterly Report, July-September 1978," SAND79-0359, NUREG/CR-0661, Sandia National Laboratories (April 1979).

15. R. Faradich, D. R. Pederson, R. Purviance, and N. Carlson, "Interactions on Penetration of Heated UO_2 with Limestone Concrete," Proc. of the Fifth PAHR Info. Exhange Meeting, Karlsruhe, (July 1982) pp. 242-247.

16. R. Faradich and W. H. Gunther, "One-Dimensional Penetration of Molten UO_2 Into Substrate Limestone Concrete," Nuclear Technology, Vol. 50, (1980) p. 298.

17. R. M. Wong, I. Catton, and V. K. Dhir, "Solid Particle Penetration of a Melting Substrate," Proc. of the Fifth PAHR Info. Exhange Meeting, Karlsruhe, (July 1982) pp. 248-250.

18. S. Z. Ahmed and V. K. Dhir, "On the Simulation of Penetration of Solidified Core Material Into Concrete," Proc. of the International Mtg. on LWR Severe Accident Evaluation, Cambridge, MA, (August 1983) pp. 12.9-1-12.9-7.

19. "Light Water Reactor Safety Research Program Quarterly Report, April-June 1978," SAND78-1901, NUREG/CR-0422, Sandia National Laboratories (April 1979).

20. W. W. Tarbell, D. R. Bradley, and F. E. Arellano, "Sustained Concrete Attack by Low Temperature, Fragmented Core Debris," SAND82-2476, NUREG/CR-3024, Sandia National Laboratories (to be published).

21. V. K. Dhir, I. Catton and J. Castle, "Role of Taylor Instability on Sublimation of a Horizontal Slab of Dry Ice," Journal of Heat Transfer, Vol. 99, No. 3, (August 1977) p. 411.

22. H. Alsmeyer, L. Barleon, J. Koster, I. Michael, V. Miller, and M. Reiman, "A Model Describing the Interaction of a Core Melt with Concrete," NUREG/TR-0039 (translation of KfK2395, Kernforschungzentrum Karlsruhe), (September 1978).

23. F. G. Blottner, "Hydrodynamics and Heat Transfer Characteristics of Liquid Pools with Bubble Agitation," SAND79-1132, NUREG/CR-0944, Sandia National Laboratories (November 1979).

24. M. Lee, M. S. Kazimi, and G. Brown, "A Heat Transfer Model for the Corium/Concrete Interface," Proc. of the International Mtg. on LWR Severe Accident Evaluation, Cambridge, Mass., (August 1983) pp. 12.6-1-12.6-7.

25. W. B. Murfin, "A Preliminary Model for Core/Concrete Interactions," SAND77-0370, Sandia National Laboratories August, 1977.

26. M. Reimann and W. B. Murfin, "The WECHSL Code: A Computer Program for the Interaction of Core Melt and Concrete," KfK2890, Kernforschungszentrum Karlsruhe (1981).

27. P. J. Berenson, "Experiments on Pool-Boiling Heat Transfer, "International Journal of Heat and Mass Transfer, Vol. 5, (1962) pp. 985-999.

28. L. Baker, et. al., "Thermal Interactions of a Molten Core Debris Pool with Surrounding Structural Materials," Proc. of the International Mtg. on Fast Reactor Safety Technology, Seattle (August 1979).

29. A. Hunsbedt, S. T. Lam, E. L. Gluekler, and F. B. Cheung, "Comparison of Melt Penetration Models," Proc. of the Fifth PAHR Info. Exhange Meeting, Karlsruhe, (July 1982) pp. 258-263.

30. S. H. Emerman and D. L. Turcotte, "Stokes' Problem with Melting," International Journal of Heat and Mass Transfer, Vol. 26, (1983) pp. 1625-1630.

31. B. D. Turland, "Growth of a Hemispherical Melt-Pool Following a Core Meltdown", CLM/RR/S2/29, Culham Laboratory, Abingdon, Oxon, England (January 1978).

32. J. V. Beck and R. L. Knight, "User's Manual for USINT," SAND79-1694, NUREG/CR-1375, Sandia National Laboratories (May 1980).

33. M. L. Corradini, "A Transient Model for the Ablation and Decomposition of Concrete," Nuclear Technology, Vol. 62, 62, (September 1983) pp. 263-273.

34. "Light Water Reactor Safety Research Program Quarterly Report, April-June 1980," SAND80-1304/2 of 4, NUREG/CR-1509/2 of 4, Sandia National Laboratories (October 1980).

35. R. K. Cole, "A Crust Formation and Refreezing Model for Molten-Fuel/Coolant Interaction Codes," Proc. of the International Mtg. on LWR Severe Accident Evaluation, Cambridge, Mass., (August 1983) pp. 12.5-1-12.5-5.

36. R. E. Henry, "A Model for Core-Concrete Interactions," Proc. of the International Mtg. on LWR Severe Accident Evaluation, Cambridge, Mass., (August 1983) pp. 12.10-1-12.10-8.

37. A. J. Suo-Antilla, "SLAM-A Sodium Limestone Concrete Ablation Model," SAND83-7114, NUREG/CR-3379, Sandia National Laboratories, (December 1983).

38. D. H. Nguyen, et. al., "Sodium-Concrete Reaction Model Development," Proc. of the Fast Reactor Safety Mtg., Lyon, France, Vol. 3 (July 1983), pp. 91-107.

39. E. R. Copus, "Development of the Inductive Ring Susceptor Technique for Sustaining Oxide Melts," SAND82-2546, NUREG/CR-3043, Sandia National Laboratories (September 1983).

40. J. T. Brittel, L. H. Sjodahl, and J. F. White, "Steam Oxidation Kinetics and Oxygen Diffusion in UO_2 at High Temperatures," American Ceramic Society Journal, Vol. 52, (1969) pp. 446-451.

41. K. Heindlhofer and B. M. Larsen, "Rates of Scale Formation on Iron and a Few of Its Alloys," Trans. of the American Society of Steel Treating, Vol. 21, (1933) pp. 865-895.

42. J. T. Brittel, L. H. Sjodahl, and J. F. White, "Oxidation of 304L Stainless Steel by Steam and by Air", Corrosion, Vol. 25, No. 1, (January 1969) pp. 7-14.

43. L. Baker, "Hydrogen-Generating Reactions in LWR Severe Accidents," Proc. of the International Mtg. on LWR Severe Accident Evaluation, Cambridge, Mass., (August 1983) pp. 16.1-1-16.1-8.

44. "Geoscience Department 1540, Quarterly Report, January 1 to March 31, 1983," Sandia National Laboratories (April 1983).

45. J. V. Beck, "Criteria for Comparison of Methods of Solution of the Inverse Heat Conduction Problem," Nuclear Engr. and Design, Vol. 53, (1979) pp. 11-22.

46. C. A. Tudbury, "Basics of Induction Heating," J. F. Rider, New York (1960).

47. D. A. Powers and J. E. Brockmann, "Release of Fission Products and Generation of Aerosols Outside the Primary System," Radionuclide Release Under Specific LWR Accident Conditions, Vol. 1, BMI-2104, Battelle Columbus Laboratory (January 1983).

48. D. A. Powers, "A Review of Steam Oxidation of Steels," Proceedings of the Workshop on the Impact of Hydrogen on Water Reactor Safety, NUREG/CR-2017, SAND81-0661, Sept. 1981.

49. D. R. Stull and H. Prophet, JANAF Thermochemical Tables, Second Edition, NSRDS-NBS 37, National Burueay of Standards Reference Data Series (June 1971).

Appendix A

Concrete Composition

Since reactor concretes are generally made using whatever local aggregates are available, their chemical compositions vary greatly. Concretes which use calcareous aggregates such as limestone ($CaCO_3$) or dolomite ($CaCO_3.MgCO_3$) are characterized by a high CO_2 content and a high liquidus temperature. Concretes with siliceous aggregates (high SiO_2 content) such as basalt have very little CO_2 and a much lower liquidus temperature. Some additional reactor concretes combine both calcareous and siliceous aggregates. One such concrete which uses limestone for a coarse aggregate and sand for a fine aggregate, and has intermediate properties, will be used as the primary test concrete in the Hot Solid experiments. Both basaltic and limestone concretes will be used later to verify the analytical models.

Tables A.I and A.II present the chemical compositions and important properties for the three concretes of interest. Note that the water content (both evaporable and chemically bound) of the three is essentially the same - varying only between four and five percent, while the carbon dioxide content varies from less than 2 percent for basaltic concrete to 35.7 percent for limestone concrete. Since these gases are released when the concrete is heated (first the evaporable water, then the bound water, and finally the carbon dioxide), there is a large reduction in the density of the limestone concrete during heating but only a small reduction in the basaltic concrete density. Also, since energy is required to liberate the CO_2, the corresponding enthalpies of decomposition for the two concretes with limestone aggregate are much greater than for the basaltic concrete. Finally, note that the liquidus temperature for the limestone concrete is much higher than the liquidus temperatures of either of the other two concretes; and it is also higher than the melting temperature of either stainless steel (1700K) or a mild steel (1790K). For this reason, the limestone concrete will only be used with the UO_2-ZrO_2 debris.

Table A.I

Chemical Compositions of the Concretes Used in the Hot Solid Tests[11]

Oxide	Basaltic Concrete	Limestone Concrete	Limestone/ Common Sand Concrete
SiO_2	54.73	3.60	35.70
CaO	8.80	45.40	31.20
Al_2O_3	8.30	1.60	3.60
MgO	6.20	5.67	0.48
Fe_2O_3	6.25	1.20	1.44
K_2O	5.38	0.68	1.22
TiO_2	1.05	0.12	0.18
Na_2O	1.80	0.08	0.82
MnO	-	0.01	0.03
Cr_2O_3	-	0.004	0.014
H_2O	5.00	4.10	4.80
CO_2	1.50	35.70	22.00

Table A.II

Properties of the Concretes[11]

Property	Basaltic Concrete	Limestone Concrete	Limestone/ Common Sand Concrete
Bulk Density (g/cc)	2.26	2.40	2.34
Free Water (wt.%)	2.90	2.30	2.70
Enthalpy* of Free Water Loss (J/g)	84.30	66.80	81.60
Bound Water (wt.%)	2.00	1.80	2.00
Enthalpy* of Bound Water Loss (J/g)	120.00	109.00	120.00
Carbon Dioxide (wt.%)	1.50	35.70	22.00
Enthalpy* of Carbon Dioxide Loss (J/g)	66.00	1560	962
Melting Temperature Range (K)	1350-1650	1720-1920	1420-1670
Enthalpy* of Melting (J/g)	550	760	500

*All enthalpies are reported per unit mass of virgin concrete.

Appendix B

Raw Data from HSS-1 and HSS-3

Data is given for HSS-1 and HSS-3 in groups according to location. All thermocouples were chromel-alumel (Type K) with the exception of channels 29 and 30 in HSS-3 which were platinum-rhodium (Type S). Each thermocouple was referenced to 0°C. The observed data scatter was due primarily to three sources:

(1) Thermocouple location which is best known to within 2 mm axially or radially.

(2) Concrete inhomogeneities due to porosity and 1.0 cm aggregate.

(3) Assymmetric erosion patterns observed in both tests.

A table is provided for each test to describe the axial, radial, and azimuthal location of the thermocouples (i.e., channels) embedded in the concrete substrate. Axial dimensions indicate the original distance from the slug/concrete interface, radial dimensions are the radius from the centerline, and azimuthal dimensions are given in degrees relative to the centerline/far radial position.

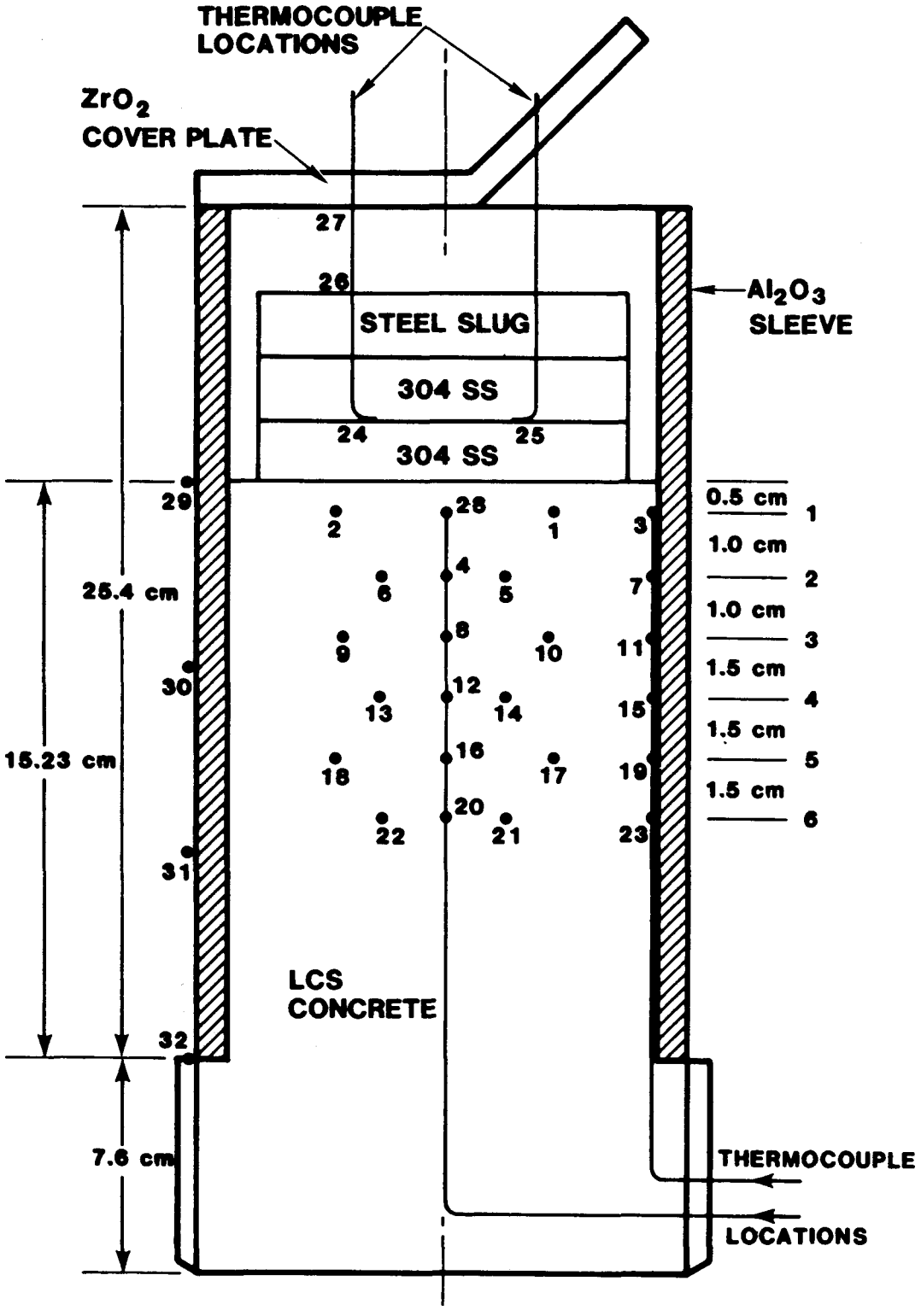

Figure B-1. HSS-1 Thermocouple Layout

Table B-1. HSS-1 Concrete Thermocouple Locations

Channel Number	Axial (cm)	Radial (cm)	Azimuthal (degrees)
28	0.5	0.	0.
1	0.5	3.8	0.
2	0.5	3.8	180.
3	0.5	7.6	0.
4	1.5	0.	0.
5	1.5	3.8	45.
6	1.5	3.8	215.
7	1.5	7.6	0.
8	2.5	0.	0.
9	2.5	3.8	90.
10	2.5	3.8	270.
11	2.5	7.6	0.
12	4.0	0.	0.
13	4.0	3.8	135.
14	4.0	3.8	305.
15	4.0	7.6	0.
16	5.5	0.	0.
17	5.5	3.8	180.
18	5.5	3.8	0.
19	5.5	7.6	0.
20	7.0	0.	0.
21	7.0	3.8	215.
22	7.0	3.8	45.
23	7.0	7.6	0.

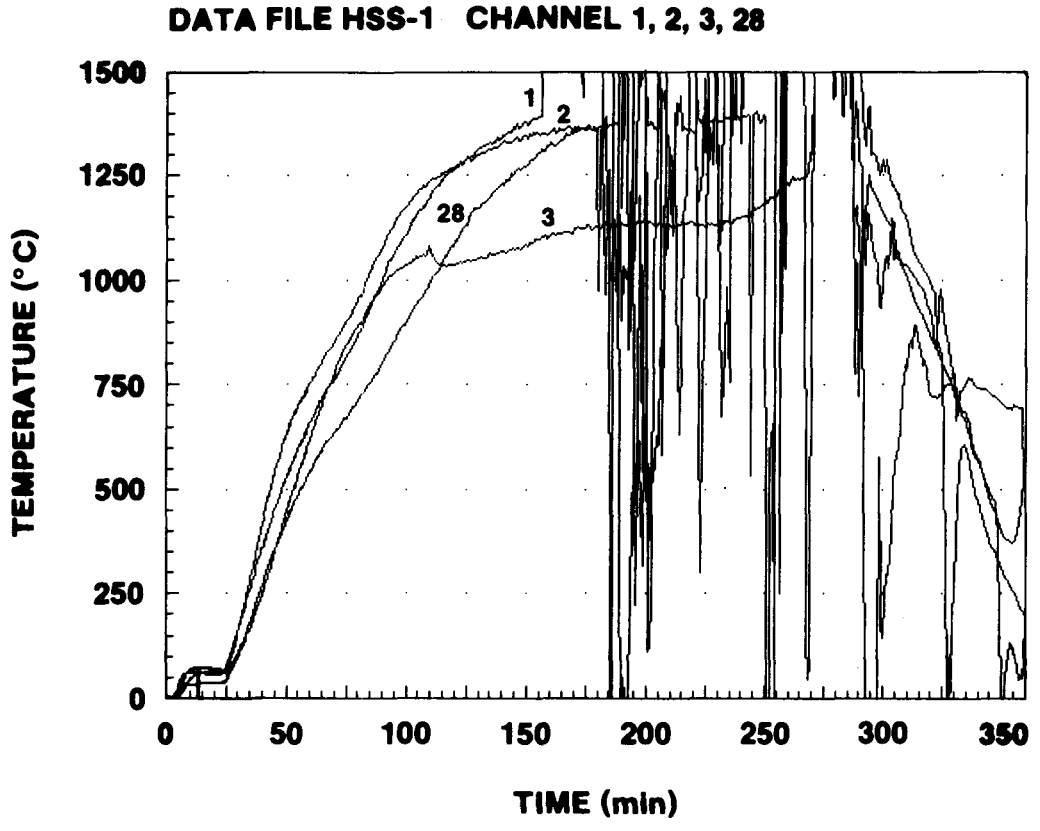
DATA FILE HSS-1 CHANNEL 1, 2, 3, 28
TEMPERATURE (°C)
1500
1250
1000
750
500
250
0
0
50
100
150
200
250
300
350
TIME (min)
1
2
28
3

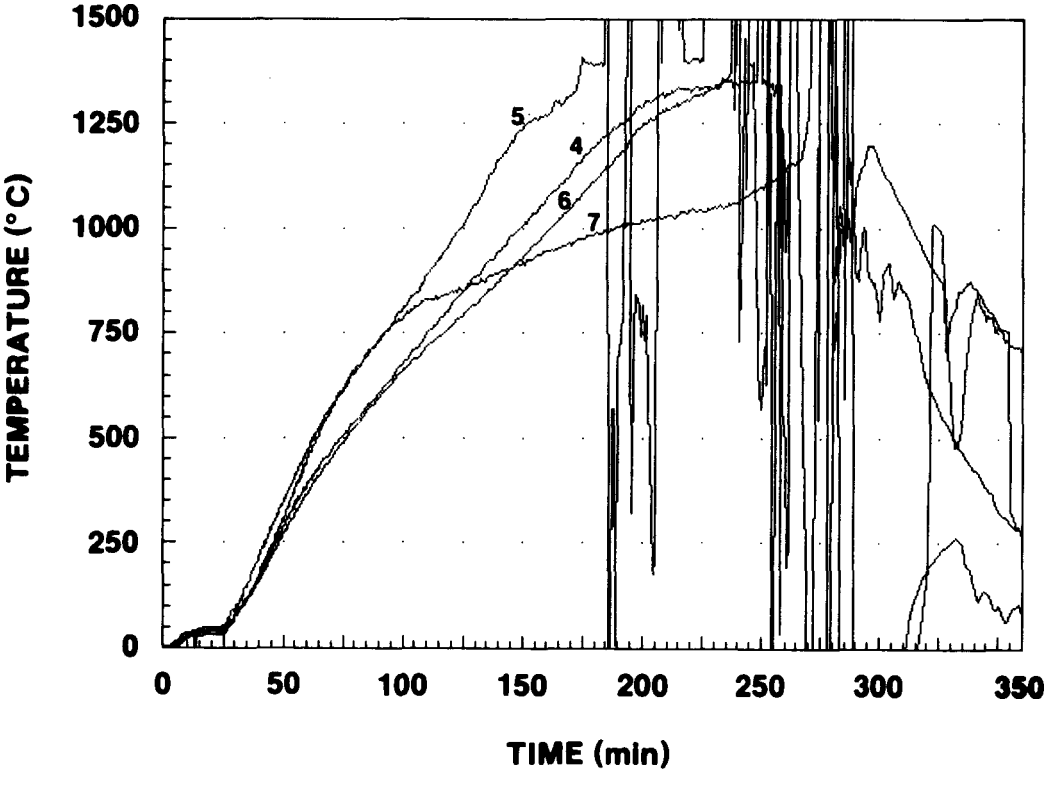
DATA FILE HSS-1 CHANNEL 4, 5, 6, 7
TEMPERATURE (°C)
1500
1250
1000
750
500
250
0
0
50
100
150
200
250
300
350
TIME (min)
5
4
6
7

DATA FILE HSS-1 CHANNEL 8, 9, 10, 11

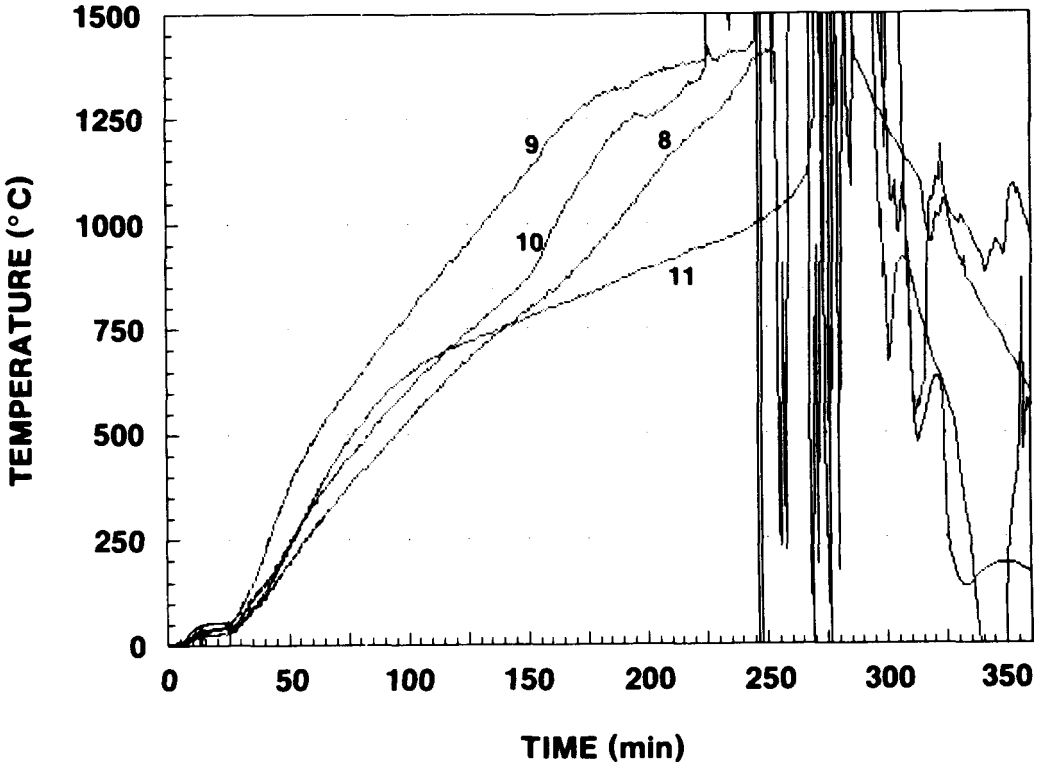

DATA FILE HSS-1 CHANNEL 12, 13, 14, 15

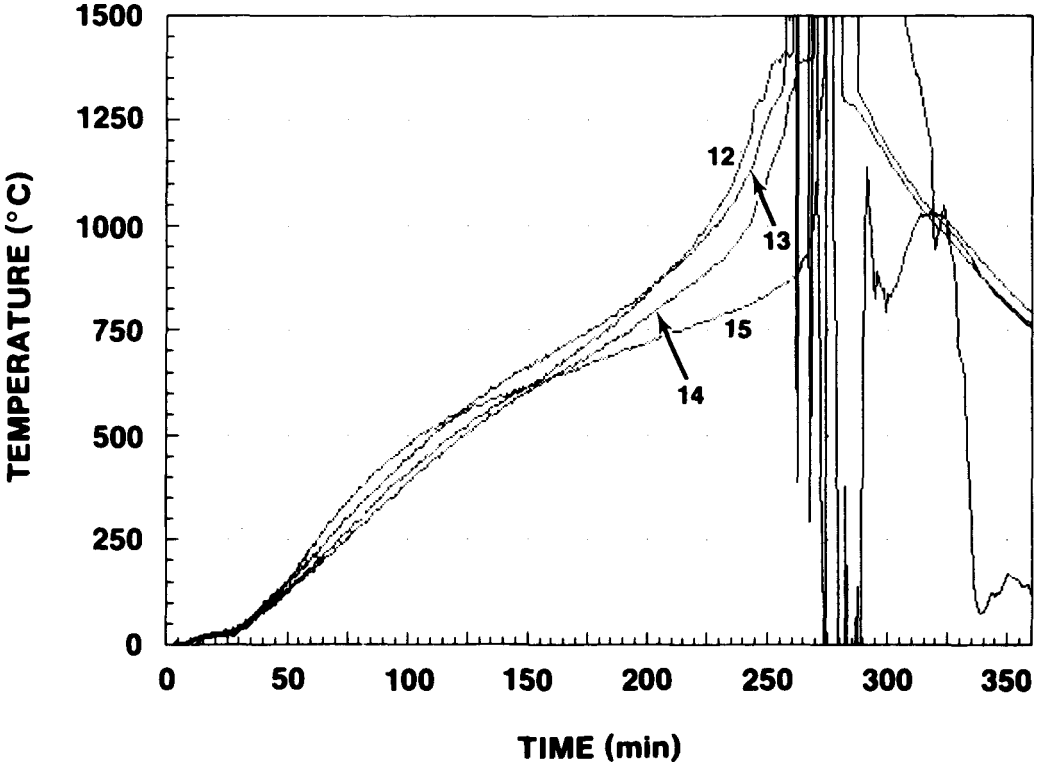

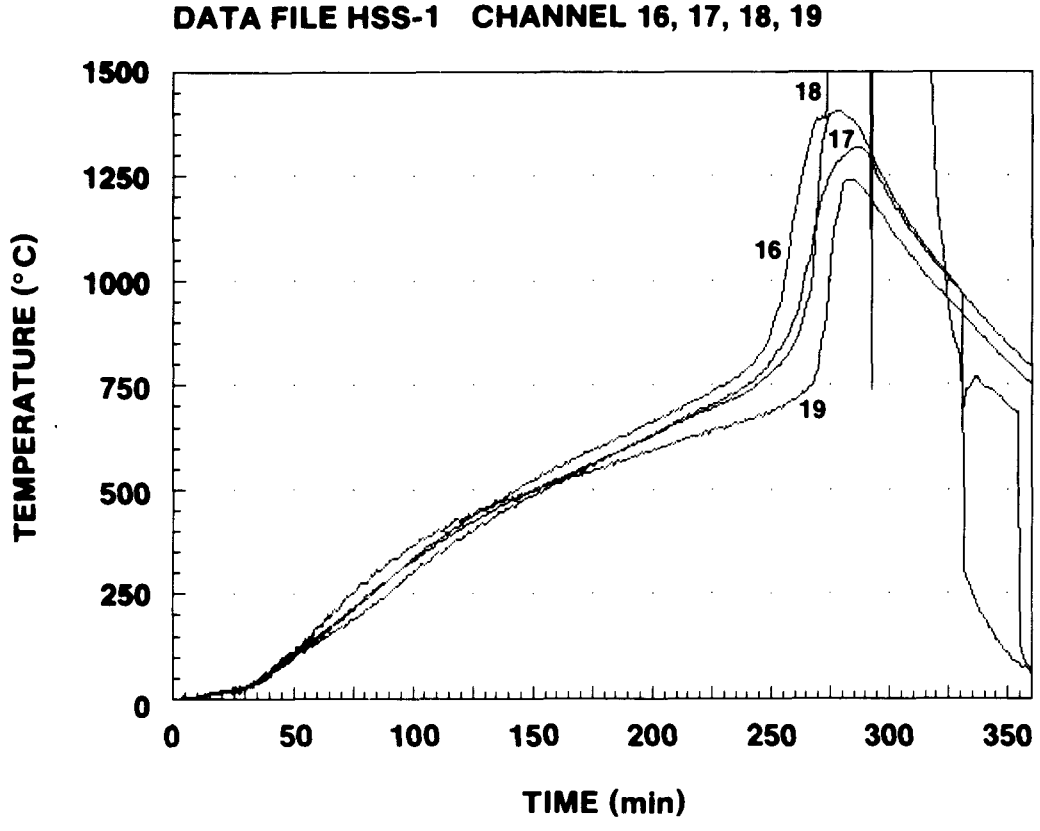
DATA FILE HSS-1 CHANNEL 16, 17, 18, 19
TEMPERATURE (°C)
1500
1250
1000
750
500
250
0
0
50
100
150
200
250
300
350
TIME (min)
18
17
16
19

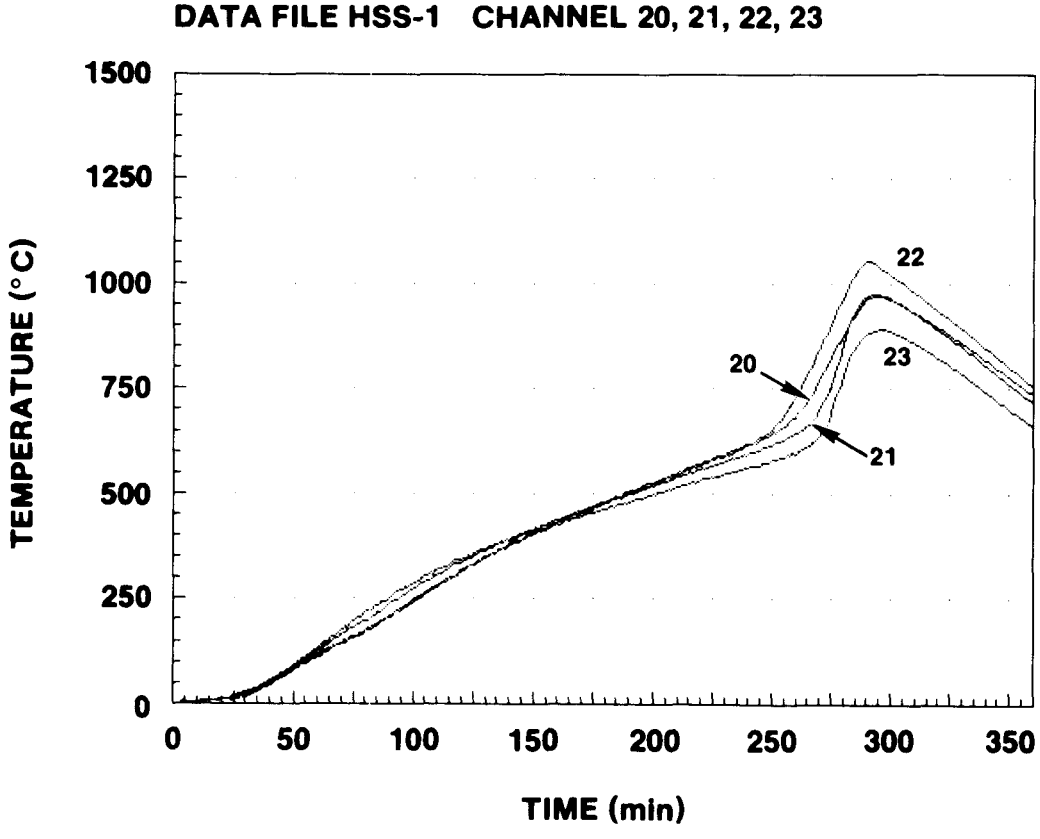
DATA FILE HSS-1 CHANNEL 20, 21, 22, 23
TEMPERATURE (°C)
1500
1250
1000
750
500
250
0
0
50
100
150
200
250
300
350
TIME (min)
22
20
23
21

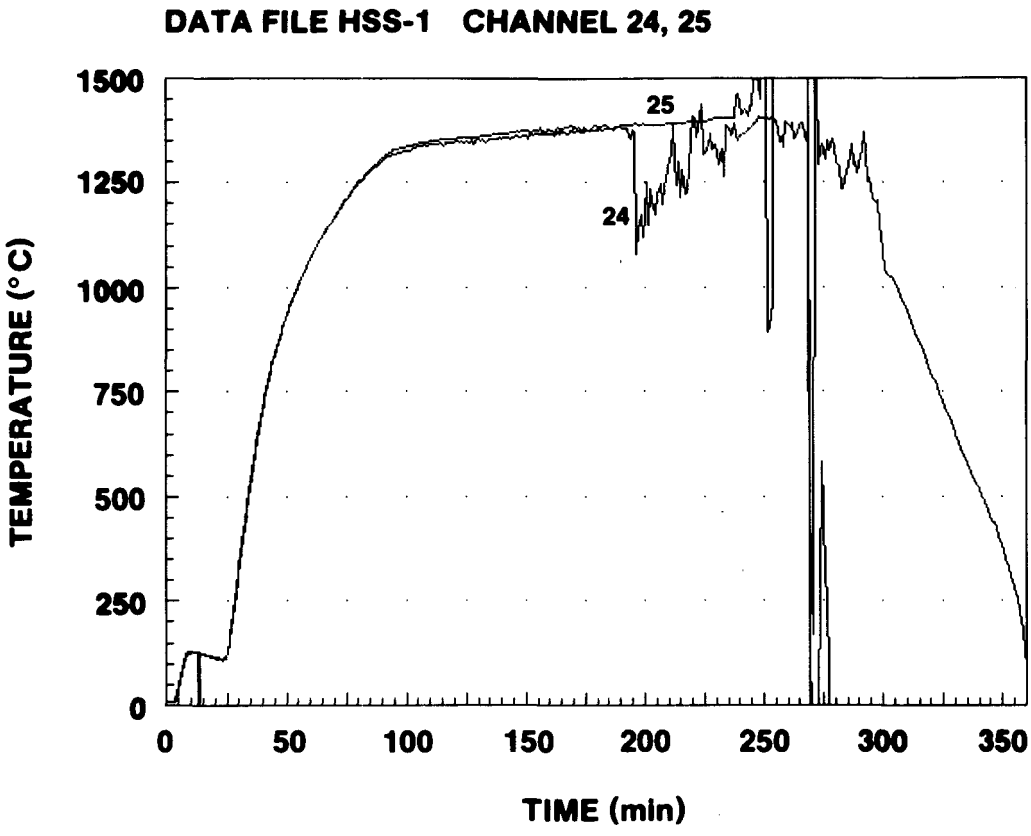
DATA FILE HSS-1 CHANNEL 24, 25
TEMPERATURE (°C)
1500
1250
1000
750
500
250
0
25
24
0
50
100
150
200
250
300
350
TIME (min)

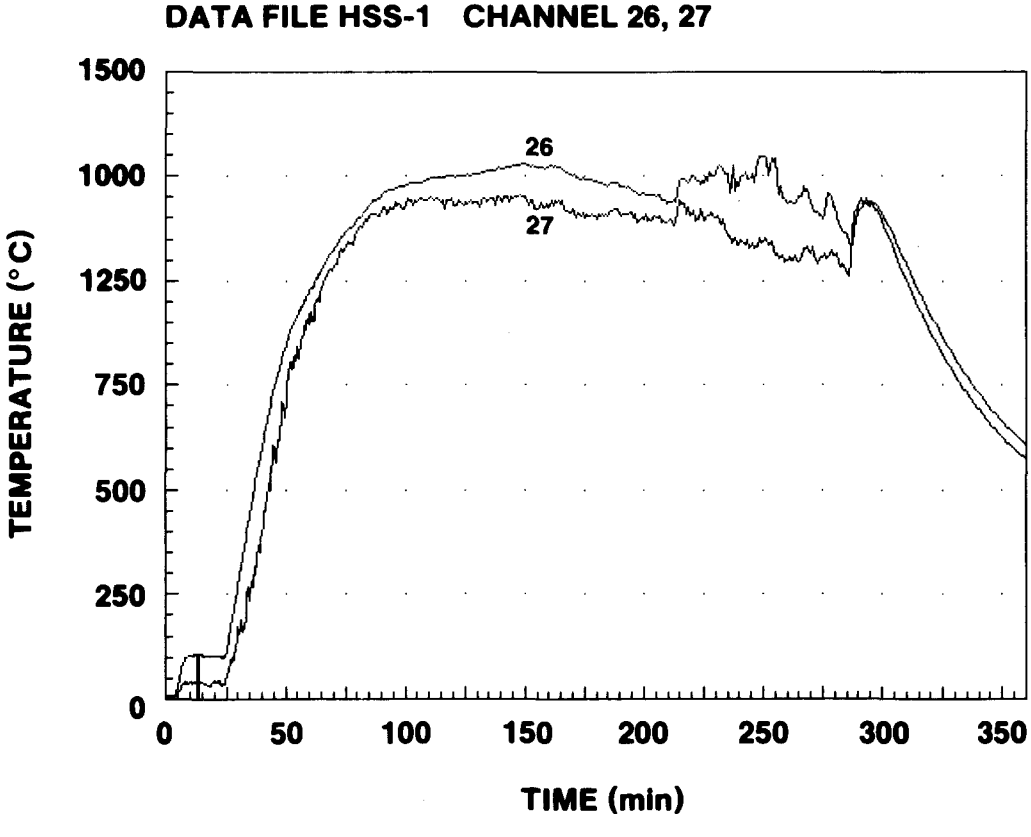
DATA FILE HSS-1 CHANNEL 26, 27
TEMPERATURE (°C)
1500
1000
1250
750
500
250
0
26
27
0
50
100
150
200
250
300
350
TIME (min)

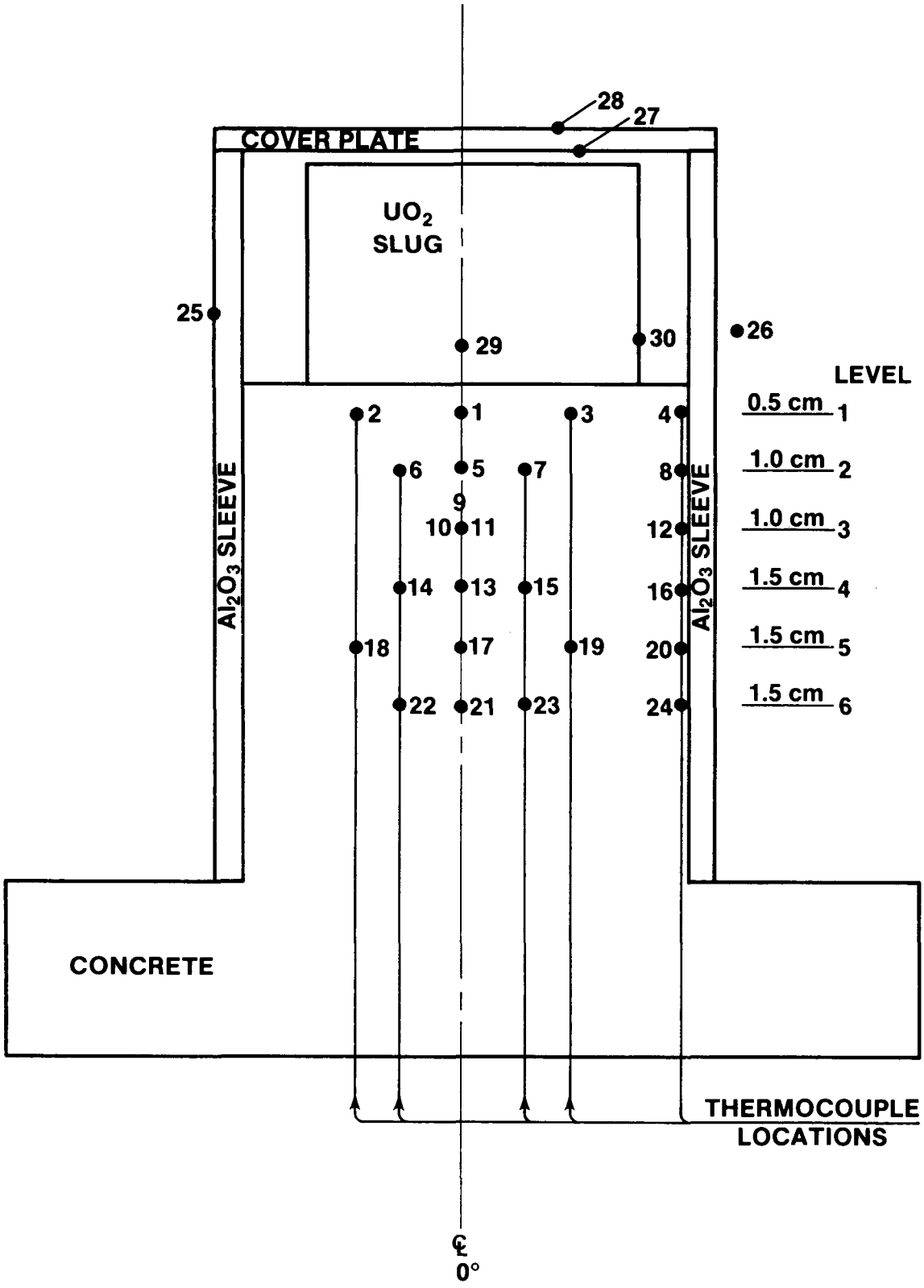

Figure B-6. HSS-3 Thermocouple Layout

Table B-2. HSS-3 Concrete Thermocouple Locations

Channel Number	Axial (cm)	Radial (cm)	Azimuthal (degrees)
1	0.5	0.	0.
2	0.5	3.8	0.
3	0.5	3.8	180.
4	0.5	7.6	0.
5	1.5	0.	0.
6	1.5	3.8	45.
7	1.5	3.8	215.
8	1.5	7.6	0.
9	2.5	0.	0.
10	2.5	3.8	90.
11	2.5	3.8	270.
12	2.5	7.6	0.
13	4.0	0.	0.
14	4.0	3.8	135.
15	4.0	3.8	305.
16	4.0	7.6	0.
17	5.5	0.	0.
18	5.5	3.8	180.
19	5.5	3.8	0.
20	5.5	7.6	0.
21	7.0	0.	0.
22	7.0	3.8	215.
23	7.0	3.8	45.
24	7.0	7.6	0.

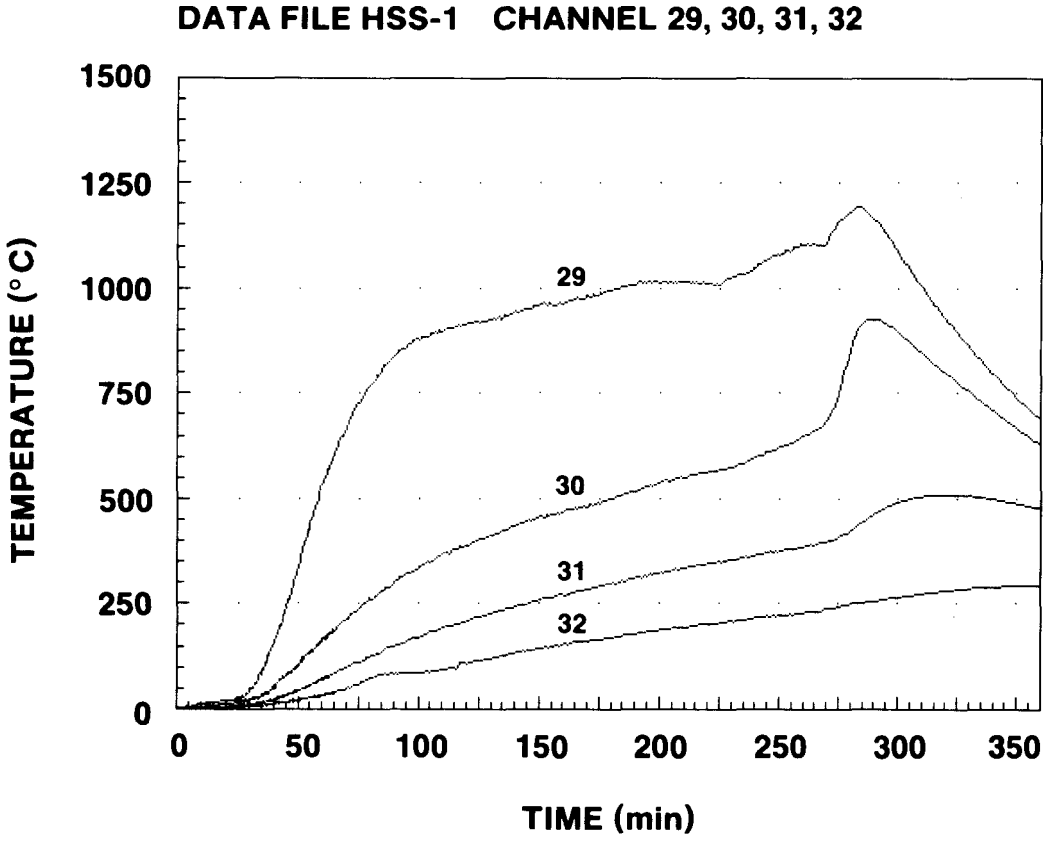
DATA FILE HSS-1 CHANNEL 29, 30, 31, 32
TEMPERATURE (°C)
1500
1250
1000
750
500
250
0
0
50
100
150
200
250
300
350
TIME (min)
29
30
31
32

DATA FILE HSS-3 CHANNEL 1, 2, 3, 4

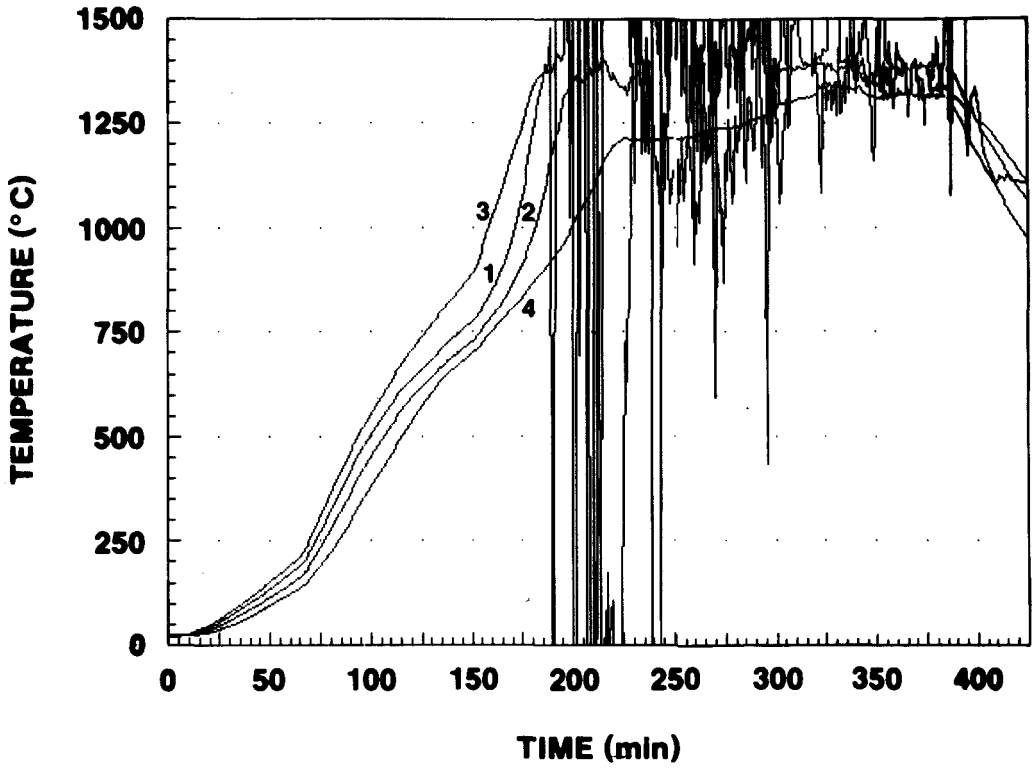

DATA FILE HSS-3 CHANNEL 5, 6, 7, 8

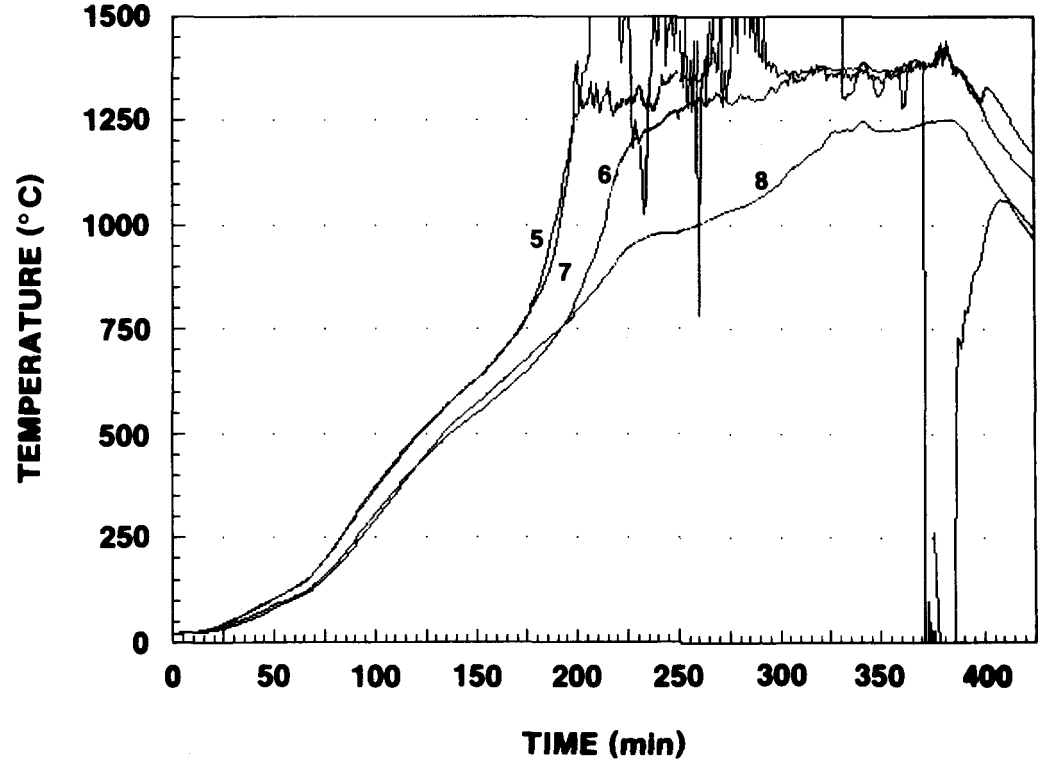

DATA FILE HSS-3 CHANNEL 9, 10, 11, 12

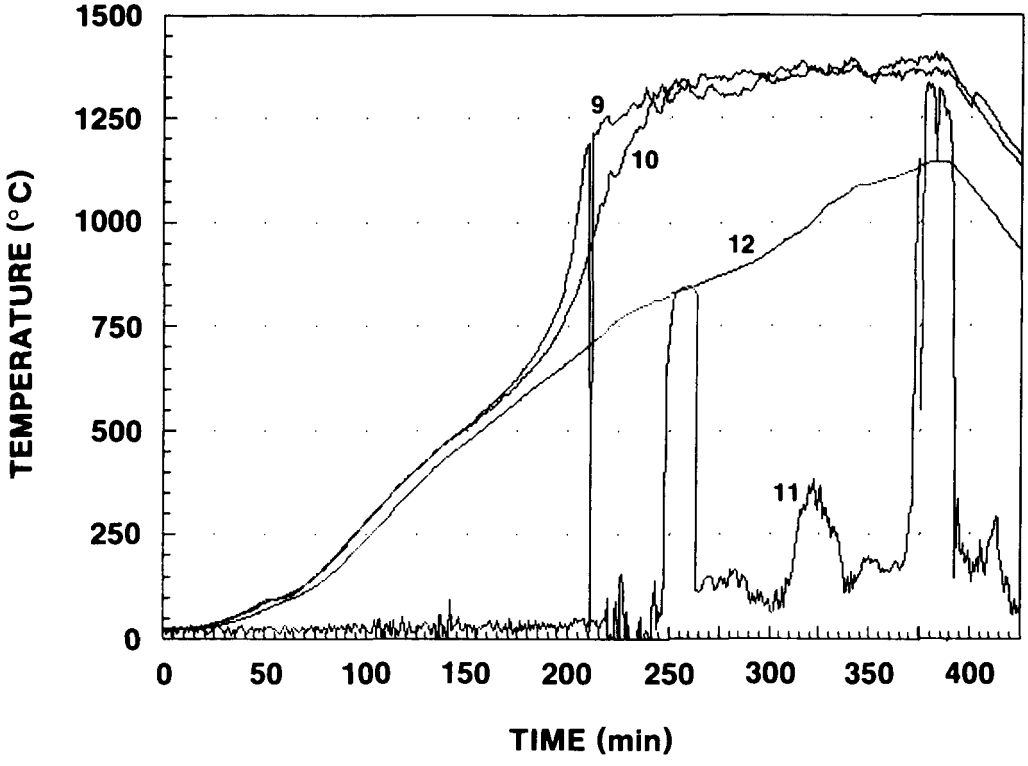

DATA FILE HSS-3 CHANNEL 13, 14, 15, 16

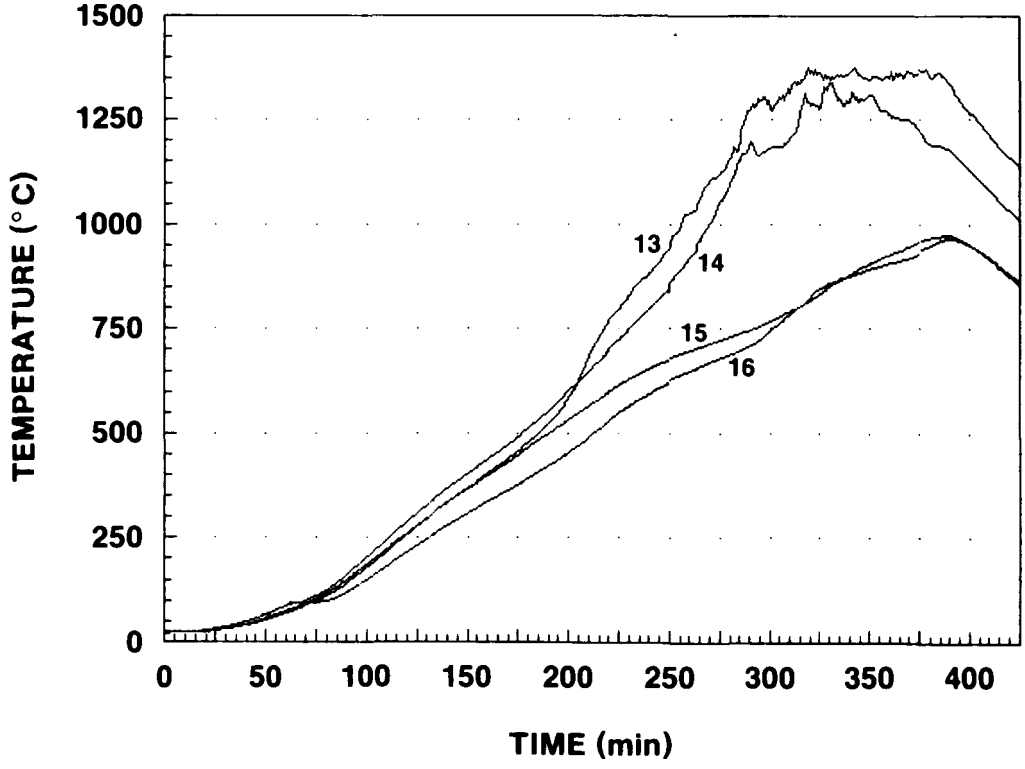

DATA FILE HSS-3 CHANNEL 17, 18, 19, 20

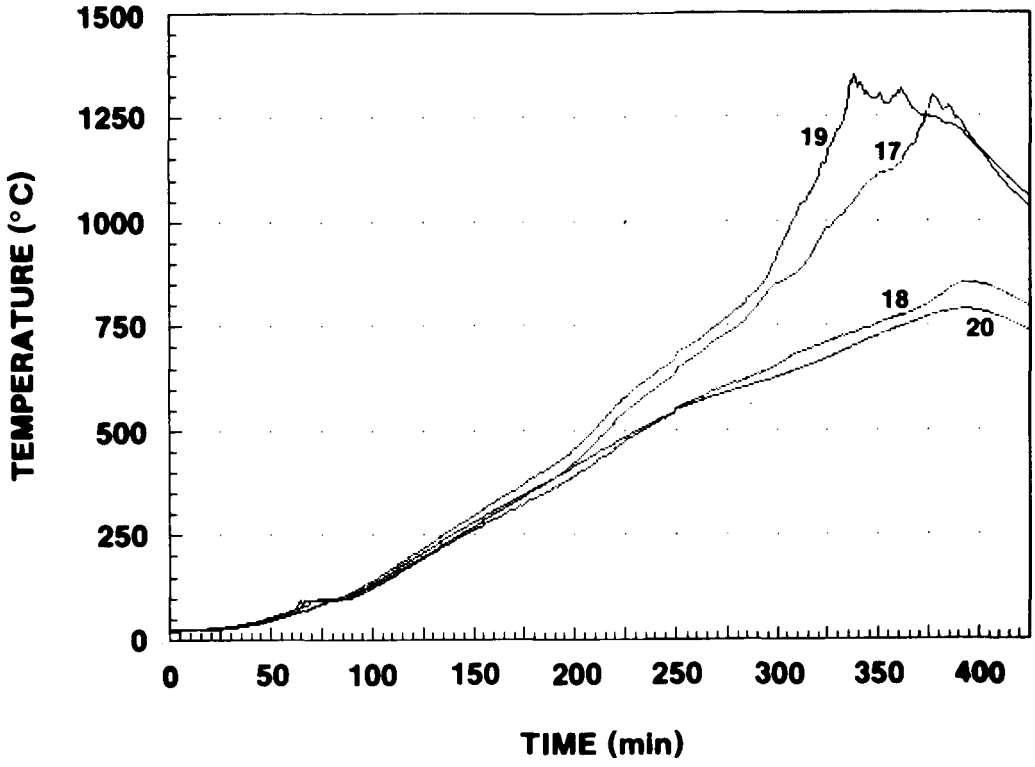

DATA FILE HSS-3 CHANNEL 21, 22, 23, 24

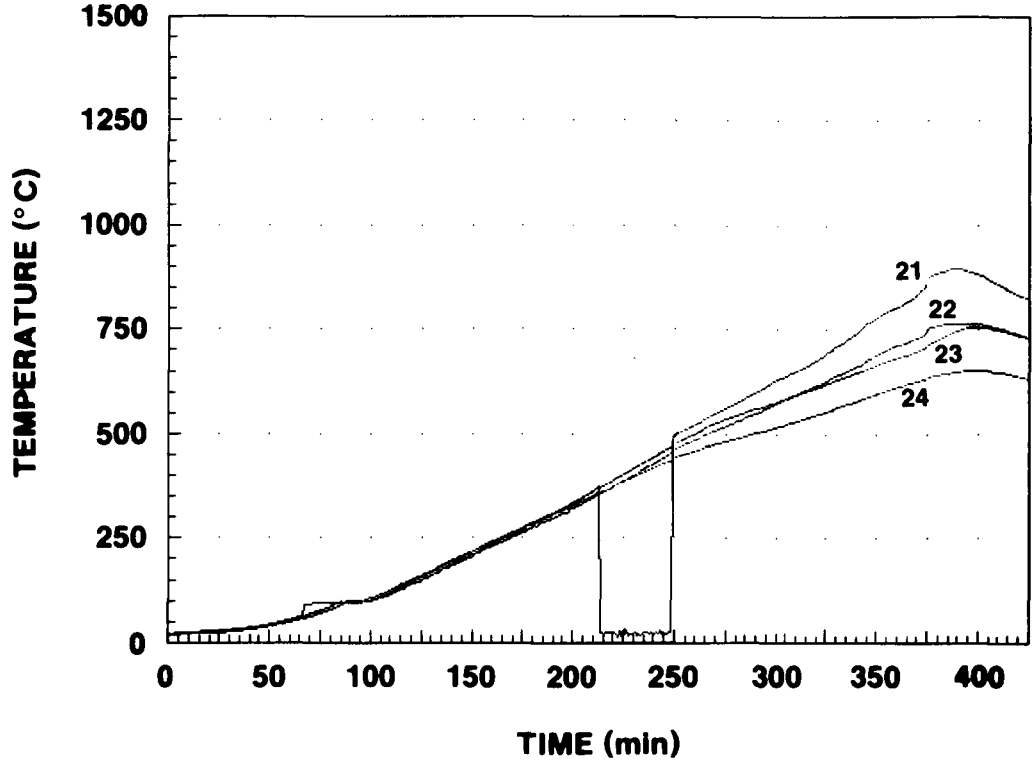

DATA FILE HSS-3 CHANNEL 25, 26, 27, 28

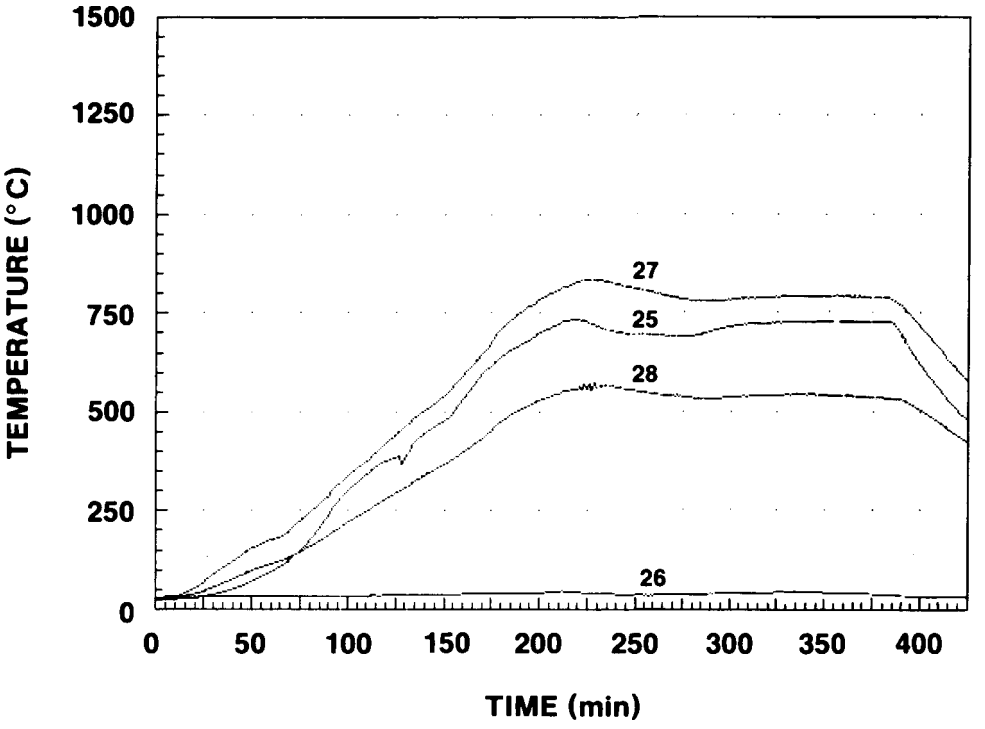

DATA FILE HSS-3 CHANNEL 29, 30

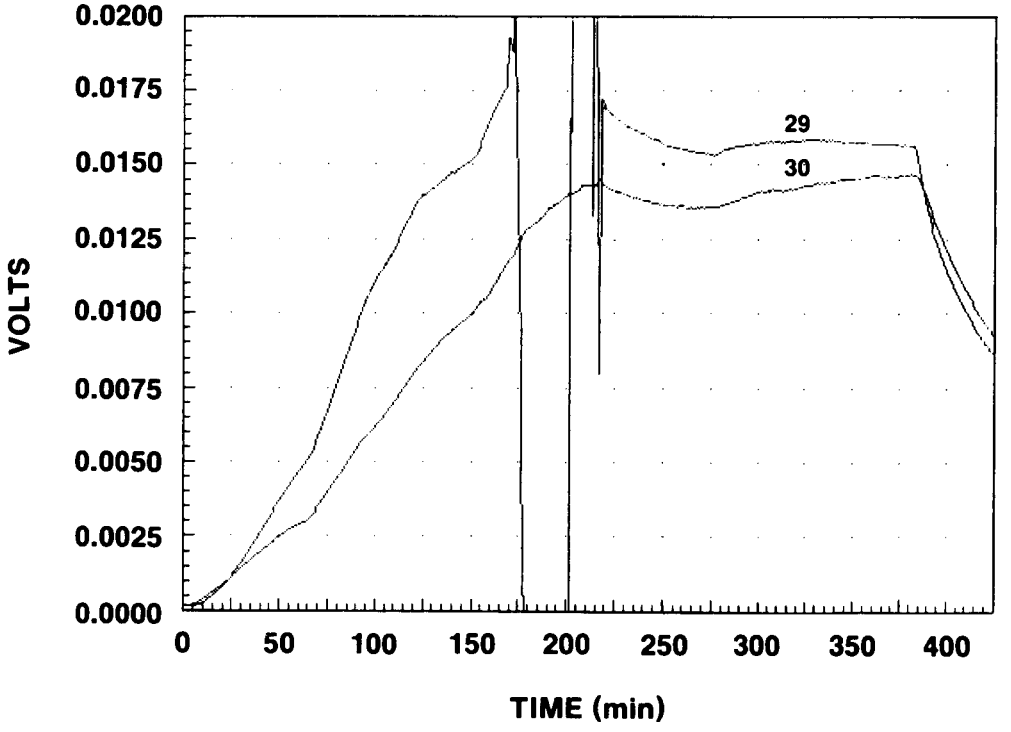

Appendix C

Material Input Parameters for HOTROX Analysis

Concrete
Parameters (same for both HSS-1 and HSS-3)

Density	- 2308 kg/m^3
Composition	- 55% $CaCO_3$ - 44% SiO_2
Specific Heat	- 1320 J/kg-°C
Conductivity	- 2.4 - .0012 T(°K) w/m-°K
Melt Point	- 1570 °K
Water Content	- 2.2% bound - 2.7% unbound

Hot Solid Parameters		(HSS-1)	(HSS-3)
Initial Temperature	-	491°K	351°K
Mass	-	9 kg	10 kg
Diameter	-	.1397 m	.13 m
Composition	-	100% Fe	95% UO_2-5% Fe
Emissivity	-	.4	.5